FINAL REPORT

Multimodal Freight Distribution to Support Increased Port Operations

Date: October, 2016

Wayne Talley, PhD, Professor & Eminent Scholar, Old Dominion University
ManWo Ng, PhD, Assistant Professor, Old Dominion University
Mecit Cetin, PhD, Associate Professor, Old Dominion University
Hesham A. Rakha, PhD, Professor, Virginia Tech Transportation Institute
Byungkyu Brian Park, PhD, Associate Professor, University of Virginia

Prepared by:
Old Dominion University, Norfolk, VA 23529
Virginia Tech, Blacksburg, VA 24061
University of Virginia, Charlottesville, VA 22903

Prepared for: MATS UTC

1. Report No.	2. Government Accession No.	3. Recipient's Catalog No.
4. Title and Subtitle Multimodal Freight Distribution to Support Increased Port Operations		**5. Report Date** **6. Performing Organization Code**
7. Author(s) Wayne Talley, ManWo Ng, Mecit Cetin, Hesham A. Rakha, and Byungkyu Brian Park		**8. Performing Organization Report No.**
9. Performing Organization Name and Address Old Dominion University, Virginia Tech, and University of Virginia		**10. Work Unit No. (TRAIS** **11. Contract or Grant No.** DTRT13-G-UTC33
12. Sponsoring Agency Name and Address US Department of Transportation Office of the Secretary-Research UTC Program, RDT-30 1200 New Jersey Ave., SE Washington, DC 20590		**13. Type of Report and Period Covered** Final 11/01/14 – 9/30/16 **14. Sponsoring Agency Code**

15. Supplementary Notes

16. Abstract
To support port operations, three different aspects of multimodal freight distribution are investigated: (i) Efficient load planning for double stack trains at inland ports; (ii) Optimization of a multimodal network for environmental sustainability; and (iii) Fuel consumption and emissions models for heavy duty diesel trucks. The report includes sections describing model development and case studies or numerical examples for these aspects. Mathematical models for solving the optimization problems are presented. For the container loading problem, a hypothetical case study with various scenarios is presented to show how maximum utilization rate is affected as the distributions of container weights and types are varied. For the optimization of a multimodal network problem, it is shown that the proposed model can save cost up to 6.3% over the comparison model and up to 21.3% over the state-of-the-art model. For the fuel consumption and emissions modeling, the predictions of the developed models for heavy duty diesel trucks are shown to be consistent with field measurements.

17. Key Words	18. Distribution Statement
Port operations, double stack trains, multimodal networks, fuel consumption, emission modeling, heavy duty diesel trucks.	No restrictions. This document is available from the National Technical Information Service, Springfield, VA 22161

19. Security Classif. (of this report)	20. Security Classif. (of this page)	21. No. of Pages	22. Price
Unclassified	Unclassified	58	

Acknowledgements

This project was partially funded by Mid-Atlantic Transportation Sustainability Center – Region 3 University Transportation Center (MATS UTC). The authors from Virginia Tech would like to thank University of California, Riverside researchers for providing with the field data in support of this research effort.

Disclaimer

LIST OF FIGURES

LIST OF TABLES

EXECUTIVE SUMMARY

To support improved port operations, three different aspects of multimodal freight distribution are investigated: (i) Efficient load planning for double stack trains at inland ports; (ii) Optimization of a multimodal network for environmental sustainability; and (iii) Fuel consumption and emissions models for heavy duty diesel trucks. The report includes three major sections describing these three aspects.

Decisions on the loading order for double stack trains are difficult to make, especially when a human operator has to decide quickly which slot a container should fill. In this project, we examine the loading of containers on a double stack train at an inland port that is destined for a seaport. Particularly, we develop a model to support the assignment of containers to rail cars, in order to maximize the utilization of the available space on the train. Not only is this critical from a resource utilization perspective, but it is particularly important for an inland port that typically has limited space for container storage (i.e., getting as many containers out of the yard per train is important) and limited rail tracks (i.e., inland ports can service a limited number of trains per day). The overall problem is formulated as a mathematical optimization problem where two types of containers are considered: 20 and 40 foot containers. In the problem formulation, the weight capacity restrictions of the railcars are enforced. A case study with various scenarios is presented to show how maximum utilization rate is affected as the distributions of container weights and types are varied.

In the second section, a multimodal freight dispatching tool is proposed. The highlights of this new dispatching tool include that (i) environmental costs are considered in addition to the transportation costs to support environmentally conscious decisions; (ii) all three types of economies — economies of scale for quantity (EOQ), economies of scale for vehicle size (EOVS) and economies of scale for distance (EOD) — are incorporated; (iii) ensures system optimal dispatching solution; (iv) easy to use for practitioners. The proposed model was evaluated in terms of total cost, transportation cost and environmental cost. Sensitivity analysis was conducted with regard to various demands, and the results prove that the proposed model outperforms both the state-of-the-art model and the comparison model which combines the state-of-the-art model with environmental consideration. The proposed model saves cost up to 6.3% over the comparison model and up to 21.3% over the state-of-the-art model, which varies based on demand. Detailed investigation revealed that the proposed model has no adverse effect on both transportation cost and environmental cost.

In the third section, fuel consumption and emissions models for heavy duty diesel vehicles (HDDVs) are developed and tested. Heavy-duty vehicles (HDVs) are the second largest source of greenhouse gas (GHG) emissions and energy use within the transportation sector even though they represent only a small portion of on-road vehicles. Heavy-duty diesel vehicles (HDDVs) emit around half of on-road nitrogen oxide (NOx) emissions. The majority of microscopic emission models suffer from two major limitations: they result in a bang-bang control system, and the calibration of model parameters is not viable using publicly available data. The Virginia

Tech Comprehensive Power-Based Fuel Consumption Model (VT-CPFM) is extended to overcome those two shortcomings to predict HDDV emissions for carbon monoxide (CO), hydrocarbons (HCs), and nitrogen oxides (NOx). Due to a lack of publicly available data, field measurements are used for model development. The model is calibrated for each individual truck and validated by comparing model estimates against in-field measurements as well as CMEM and MOVES model estimates. The results demonstrate that the model should be restricted to be convex, although empirical measurements do seem to point to a concave function of vehicle power, in order to provide realistic driving recommendations from the system perspective. The convex model is demonstrated to estimate fuel consumption levels consistent with in-field measurements as well as CMEM and MOVES, without significantly sacrificing the model accuracy. The optimum fuel economy cruise speed ranges between 32-52 km/h for all of the test vehicles varying the grade level from 0% to 8%, and moves towards the negative direction with an increase in the vehicle load and grade level; namely, steeper roadway grades and heavier vehicles result in lower optimum cruise speeds. The fuel predictions of the model can accurately estimate CO2 emissions, which are demonstrated to be consistent with field measurements.

I. LOAD PLANNING IN DOUBLE STACK TRAINS FOR IMPROVED EFFICIENCY

PROBLEM STATEMENT

Double stack trains are the most common means of rail transport in the United States. With a depressed platform, each well car can carry double-stacked containers while maintaining centers of gravity within acceptable heights. Double stack trains revolutionized intermodal transport of containers in the United States. The innovative double stack service was first introduced by Southern Pacific Railroad in 1977, and it became adopted by American President Lines in 1984 to improve the efficiency of container transport from Los Angeles to Chicago. Double stack trains rapidly replaced Trailer on Flat Car (TOFC) and Container on Flat Car (COFC) because of its higher efficiency, and they became the most popular type of rail transport for containers in North America. Other countries, such as Australia, China, India, and Panama have adopted double stack trains as well.

Double stack trains are used at inland ports as well. An inland port (also known as dry port in other countries in the world) is "an intermodal inland terminal directly connected to a seaports with high capacity transport means, where customers can leave/pick up their standardized units as if directly to a seaport" [1]."The concept of the dry port is based on a seaport directly connected by rail with inland intermodal terminals, where shippers can leave and/or collect their goods in intermodal loading units as if directly at the seaport" [2].

In addition to providing transshipment cargo service, a dry port may also provide other such cargo services as storage, consolidation and customs clearance as well as vehicle services such as vehicle repair and maintenance. In China, "customs clearance is the core function of dry ports" [3]. "Dry ports have been widely implemented worldwide: typical examples including Eskilstuna Dry Port in Sweden, Kansas City and Virginia Inland Port in US, Isaka Dry Port in Tanzania and Xian Dry port in China" [4].

Inland ports are special from a rail load planning perspective in the sense that there is only one destination, i.e. the seaport, for its outbound (double stack) trains. In this study, we examine the loading of containers on a double stack train at an inland port that is destined for a seaport. Particularly, we develop a model to support the assignment of containers to rail cars, in order to maximize the utilization of the available space on the train. Not only is this critical from a resource utilization perspective, but it is particularly important for an inland port that typically has limited space for container storage (i.e. getting as many containers out of the yard per train is important) and limited rail tracks (i.e. inland ports can service a limited number of trains per day).

RESEARCH APPROACH

While research exists on loading single stack rail cars, limited work has been done for double stack trains. Below is a summary of a sample of research in this area.

A Decision Support System to Load Containers to Double-Stack Rail Cars[5]

Decisions on the loading order for double stack trains are difficult to make, especially when a human operator has to decide quickly which slot a container should fill. The quality of such decisions tends to be low because of the uncertainties about the exact order and characteristics of incoming containers. Although it is possible to postpone the loading of double stack trains until all of the containers have arrived, the extra amount of time and space spent on double-handling containers make this option unattractive. The decision support system, Double Stack Planner (DSP), described in this paper incorporates information on incoming containers. Thus, it can assist the human operator in assigning containers to appropriate slots in an efficient fashion that evenly distribute weight along the train while maintaining the lowest possible centers of gravity.

DSP includes statistical constraints developed through on-site observations and various interviews with subject matter experts. In addition to the weight limit and height clearance, DSP particularly suggests assigning 20-foot or heavy 40-foot containers to the bottom and light 40-foot containers to the top. An even weight distribution is an important safety feature because derailment is more likely when the weight of the train is concentrated to the latter cars in the train. The goal of DSP, according to the article, is to load double stack trains in a way "that maximizes the load factor and minimizes the center of gravity and variations in truck and platform loads." DSP also has the flexibility to allow users to override the system's suggestion as long as there is no violation to the programmed constraints.

Simulation using DSP under various scenarios show positive results. Reserving slots for 20-foot containers increases the load factor and utilization of rail car. Additionally, the prioritization of loading heavier containers on the bottom can ensure lower and more uniform center of gravity. Therefore, DSP has the capability to achieve the goal of lowering the center of gravity, increasing load factor, and reducing variations in truck and platform loads. However, the load factor could decrease if many containers on the bottom are overly heavy, which limits the number of containers that can be loaded on the top due to rail car's weight capacity.

Loading Containers on Double-Stack Cars: Multi-objective Optimization Models and Solution Algorithms for Improved Safety and Reduced Maintenance Cost [6]

This study develops a model of loading double stack trains that optimizes the height of the center of gravity and load balance. The variability in double stack trains' relatively high center of gravity causes safety concerns, especially when trains take corners. From a horizontal perspective, if the center of gravity is concentrated to one end of a rail car, the other end becomes more susceptible to the dynamic forces while the train travels at high speed. These factors cause excessive stress that damages trains and rail tracks at the minimum, and perhaps even derailment. Therefore, balancing the center of gravity can improve operational safety and reduce maintenance costs.

Maintaining low centers of gravity and balancing weight distribution are a challenging goal. Although rail operators have created rules for loading double stack trains, these rules are too simplistic considering the random nature of the loading process. The optimization model described in this paper can help rail operators achieve the goal with a sophisticated method. The inputs to this model—the payload of rail car, height of the center of gravity, and difference between the loads of two rail cars—are based on conditions in China. For example, only Interbox Connector (IBC) rail cars with 20-foot and 40-foot containers are considered—bulkhead cars and other container sizes are not included because they are not used in China. However, the model can be easily adjusted for the requirements of other countries.

The optimization model includes three objectives with priorities in the following order: maximizing the load, lowering the center of gravity, and balancing the loads. The authors of this paper are able to obtain optimal solutions using three different approaches. However, a two-stage heuristic algorithm is identified as the best approach. The first stage involves matching pairs of 20-foot containers with 40-foot containers to form an initial solution. In the second stage improvement is made to the initial solution by switching the positions of containers. This approach requires the least amount of computation time; thus, it has the highest practical value.

Optimizing the Aerodynamic Efficiency of Intermodal Freight Trains[7]

This article focuses on the method of loading intermodal trains that maximizes fuel efficiency by reducing aerodynamic drag. Intermodal trains suffer from very high air resistance due to the

loads and design of rail car. For example, an intermodal train has 25% higher aerodynamic drag coefficient than a fully loaded coal train. The high air resistance when travelling at high speed—typically 70 mph—greatly reduces the fuel efficiency of intermodal trains. Previous research has found that air resistance can be decreased by 27% by improving the assignment of loads to cars, which reduces fuel consumption by 1 gallon per mile. An Aerodynamic loading assignment model (ALAM) is developed in this paper to assist rail operators in assigning containers to slots more efficiently. The model can be applied to all types of intermodal load and rail car.

The model is developed based on the route of BNSF Railway between Los Angeles and Chicago. Only about 20 percent of trains travelling on this route make one or two intermediate stops that are close to destinations; therefore, the authors consider the effect on aerodynamic performance based on only the initial loading pattern. This study is different from the other two as it takes into account not only double stack trains, but also spine-cars that have one slot per unit. The model includes two factors that affect aerodynamics: containers' positions in train and the length of gap between loads.

Aerodynamic drag increases when the gap between loads becomes larger. Furthermore, the result of wind tunnel tests indicates that aerodynamic drag declines continuously from the lead locomotive to the 10th car, from which point onward drag becomes almost constant. The authors address this phenomenon by introducing the concept of "total adjusted gap length (TAGL)"—gap length weighted by its relative position. Gaps in the front of the train are weighed more heavily than gaps in the back. For double stack trains only the upper level gap is considered. Therefore, the objective of ALAM is to assign loads with shorter gaps in the front of the train in order to minimize the TAGL. The algorithm of ALAM requires reasonably short amount of computation time; therefore, it can be used in real-world rail operations.

Several scenarios with various types of trains and containers are taken into account. When the number of containers equals the number of slots, double stack trains carrying domestic containers have the greatest potential for improvement in reducing TAGL. If the number of containers exceeds the number of slots, only double stack trains carrying international containers show little potential for improvement. However, if the number of containers is less than the number of slots, then all configurations show great potential for improvement because the calculation of TAGL ignores empty rail cars. In this scenario, the authors recommend loading all containers in the front of the trail while removing all empty units from the end. In general, assigning loads to TOFC and COFC presents the greatest opportunity to reduce TAGL and fuel consumption. By contrast, ALAM adds little benefit to assigning 20-foot and 40-foot international containers to double stack trains.

METHODOLOGY

Model Formulation

Figure 1 shows the four loading patterns for a double stack train, for 20 and 40 foot containers, the most common container sizes. For example, in Loading Pattern 1, two 40 foot containers are stacked on top of each other, whereas in Loading Pattern 2 two twenty foot containers are at the bottom of the well car and one 40 foot container on top. Clearly, Loading Patterns 1 and 2 will lead to a higher utilization of the space compared to Loading Patterns 3 and 4. Note that technically, a fifth loading pattern could be having only one twenty foot container loaded on a well car. However, since in practice the 40 foot container is much more often used than a 20 foot container, the more space efficient Loading Pattern 3 can always be used (instead of this "fifth loading pattern").

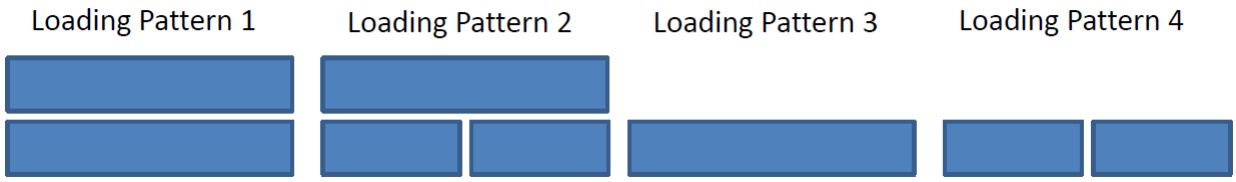

Figure 1: Loading patterns double stack train

Sets

$I = \{1,2...,m\}$	Set of 20 foot containers to be loaded on train
$J = \{1,2,...,n\}$	Set of 40 foot containers to be loaded on train
$K = \{1,2...,r\}$	Set of railcars

Parameters

w_i	Weight of 20 foot container $i \in I$
v_j	Weight of 40 foot container $j \in J$
c_k	Weight capacity of railcar $k \in K$

Decision variables

x_{ik}	Equals 1 if 20 foot container i is loaded on rail car k, 0 otherwise.
y_{jk}	Equals 1 if 40 foot container j is loaded on rail car k, 0 otherwise.
z_k	Equals 1 if there is at least one 20 foot container to be loaded on rail car j, 0 otherwise.

Objective Function and Constraints

$$\text{Max} \quad \frac{1}{4|K|}\left(\sum_{k\in K}\sum_{i\in I} x_{ik} + 2\sum_{k\in K}\sum_{j\in J} y_{jk}\right) \tag{1}$$

Subject to

$$\sum_{i\in I} x_{ik} = 2z_k, \ \forall k \in K \tag{2}$$

$$\sum_{k\in K} x_{ik} \le 1, \ \forall i \in I \tag{3}$$

$$\sum_{j\in J} y_{jk} \le 2, \ \forall k \in K \tag{4}$$

$$\sum_{j\in J} y_{jk} \le 3 - 2z_k, \ \forall k \in K \tag{5}$$

$$\sum_{k\in K} y_{jk} \le 1, \ \forall j \in J \tag{6}$$

$$\sum_{j\in J} v_j y_{jk} + \sum_{i\in I} w_i x_{ik} \le c_k, \ \forall k \in K \tag{7}$$

$$x_{ik} \in \{0,1\}, \ \forall i \in I, k \in K \tag{8}$$

$$y_{jk} \in \{0,1\}, \ \forall j \in J, k \in K \tag{9}$$

$$z_k \in \{0,1\}, \ \forall k \in K \tag{10}$$

The objective function (1) expresses the goal to maximize the utilization of the double stack train, i.e. to load as many twenty foot equivalent units (TEUs). Constraint (2) ensures that

either two 20 foot containers are loaded on railcar k, or none. Constraint (3) states that a given 20 foot container can be assigned to at most one rail car. In (4), it is ensured that the number of 40 foot containers loaded on any railcar cannot exceed two. However, if 20 foot containers are to be loaded on railcar k (i.e. $z_k = 1$), then at most one 40 foot container can be loaded on the same railcar, as dictated by constraint (5). Note that on the other hand, if $z_k = 0$, then constraint (4) will ensure that at most two 40 foot containers can be placed on the railcar. As with 20 foot containers, a given 40 foot container can be assigned to at most one rail car (6). In (7), the weight capacity restrictions of the railcars are enforced. Finally, constraints (8) to (10) state the binary nature of the decision variables.

CASE STUDY AND RESULTS

The max gross weight of containers is assumed to be 67,200 lbs. for 20 foot containers, and 71,650 lbs. for 40 foot containers [8]. The capacity of the rail cars is set at 100,000 lbs. five problem instances were randomly generated in Table 1 by varying the lower limit of the container weights. For example, in instance 1, containers weights for 20 foot containers were randomly generated from the range 10,000 lbs. to 67,200 lbs. and weights for 40 foot containers from the range 20,000 lbs. to 71,650 lbs. The lower limits are gradually increased in instances 1 to 4. In problem instance 5, instead of a uniform distribution, a normal distribution has been used to generate the container weights. For 20 foot containers, the mean was 40,000 lbs. For 40 containers, the mean was 50,000 lbs. The standard deviation was set at 10,000 lbs. for both container types.

Only 40 railcars are considered in the calculation; therefore, the double stack train can carry a maximum of 160 TEUs. For every problem instance, calculation of utilization rate begins with a pool of thirty 20-foot and eighty 40-foot containers, i.e., a total of 190 TEUs. The number of each type of containers is reduced by five for three subsequent calculations in every problem instance which helps us identify the effect on the utilization rate from having fewer containers.

By comparing the utilization rates within each column of the first four instances, one can notice that utilization rate decreases as containers become heavier. This is because the capacity of railcars is set at 100,000 lbs. and the model does not allow overloading. Consequently, utilization rate becomes 50% in Instance No. 4 when the lower bounds are increased to 50,000 lbs. for twenty-foot containers and 60,000 lbs. for 40 foot containers, each railcar can carry at most one 40-foot container.

Table 1: Train utilizations

Instance Number	**30 20's** **80 40's**	**25 20's** **75 40's**	**20 20's** **70 40's**	**15 20's** **65 40's**
1-10,000lbs/20,000lbs	100%	100%	100%	90.62%
2-20,000lbs/30,000lbs	100%	98.75%	96.25%	90.62%
3-40,000lbs/50,000lbs	54.38%	54.38%	53.75%	52.50%
4-50,000lbs/60,000lbs	50%	50%	50%	50%
5-40,000k/50,000lbs (10000)	94.37%	93.12%	92.50%	88.75%

Comparison among utilization rates within each problem instance reveals that reducing the number of available containers decreases utilization rate. Utilization rate is higher when the number of containers exceeds the available slots of a train because there are more options for matching containers to railcars. However, such options become more limited as the weights of containers increase. Figure 2 provides a visual summary of the results.

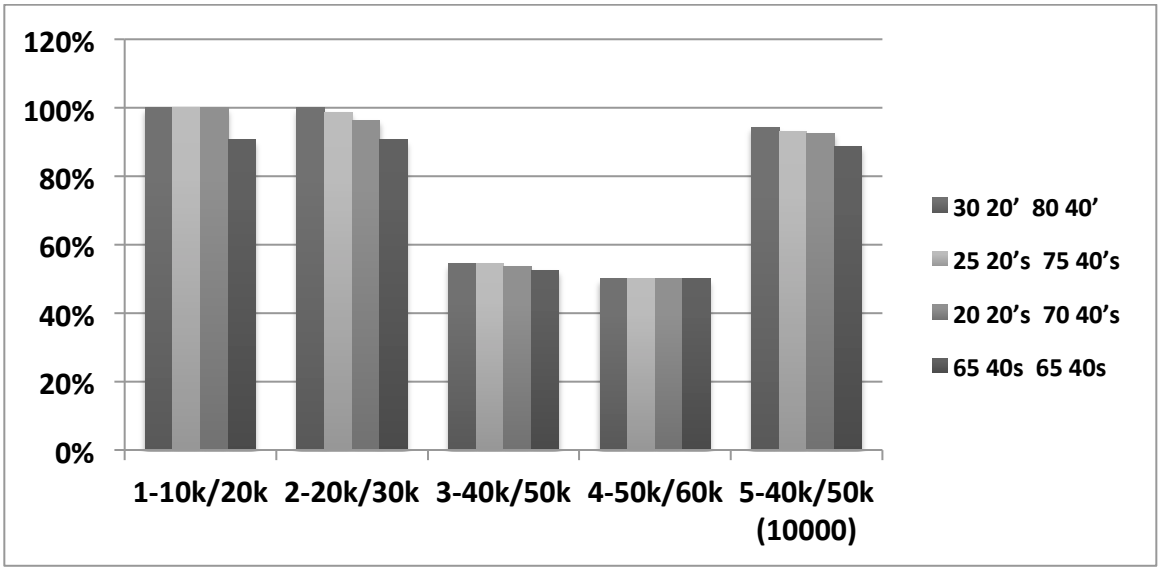

Figure 2: Summary of Results

II. OPTIMIZATION OF MULTIMODAL NETWORK SYSTEM FOR ENVIRONMENTAL SUSTAINABILITY INCORPORATING ECONOMIES OF SCALE

PROBLEM STATEMENT

It is a common practice that freight logistics systems are operated under multimodal freight system where transports are carried out by combinations of different modes of transportation systems (e.g., trucks, rails and vessels) to reduce total logistics costs. In freight transportation market, the economies of scale mainly consist of three types: economies of scale for quantity (EOQ), economies of scale for distance (EOD), and economies of scale for vehicle sizes (EOVS). Each type of economies of scale is gained through the declining unit cost over greater cargo quantity, longer haulage distance, and heavier capacity of vehicles. Such effectiveness of costs, unlike the single-mode freight system, incurs mainly through the economies of scale which represents the behavior of costs that increase less-than-proportionate to the output increase.

The economies of scale are often simplified in the existing models. Figure 3 shows two kinds of unit cost curves of various freight modes with respect to the level of cargo quantity. For visualization, the distance is assumed constant for the case of Figure 3. Figure 3-(a) is the true unit cost curve where instant jumps are observed due to discrete increase in vehicle number. Figure 3-(b) is a smoothed fitted unit cost curve which is an approximation of the true unit cost curve. The smoothed fitted unit cost is what has been widely adopted for computation simplicity [9-16]. However, this assumption sacrifices accuracy and actually could lead to incorrect optimal solution. In addition, economies of scale in the existing studies are commonly partially represented. For example, the economies of scale were implicitly considered by applying scale factors to account for taking advantage of hub facilities [17-19]. O'Kelly and Bryan [14] and Kim, et al. [13] solely considered the economies of scale for quantity (EOQ) by imposing incentives on the inter-hub links. The model developed in Sitek and Wikarek [16] explicitly considered the economies of scale for vehicle sizes (EOVS) by defining different unit costs functions for each freight modes. However, the management of multimodal freight system requires more complex dispatch model. As discussed in Jara-Dıaz and Basso [20], all the three factors including EOQ, EOD and EOVS significantly impact on marginal costs. Kim, et al. [21] also stated that different freight modes have different sensitivity towards each type of economies of scale (e.g., trucks are more likely to be distance-sensitive and vessels are more likely to be vehicle-size sensitive). Thus, considering the comprehensive components of the economies of scale is of critical in developing a freight optimization tool. In light of this perspective, the most advanced model was developed by Kim, et al. [21] who explicitly incorporated all three types of economies of scale (e.g., EOQ, EOD, and EOVS) and solved the model with Genetic Algorithm (GA). The model successfully emulated the mechanism of multimodal systems. In the Kim's model [21], however, the optimal solutions were found using a heuristic searching strategy which does not guarantee a system-wide optimal.

Another limitation of the existing models is that they do not properly consider environmental impacts. Freight companies are now subject to considering eco-friendly practices due to regulations or incentives by federal government. According to the US Environment Protection Agency report [22], the freight transportation accounts for about 10% of total greenhouse gas (GHG) emissions and 38% of the GHG emissions generated from the transportation sector in the US in 2013. This share of 38% is split into freight transportation modes as truck (22.5%), rail (2.6%) and vessels (2.2%)[22]. Another statistics reported that from 1990 to 2007, emissions from freight transportation have been continuously risen by 35% mainly

due to the increase in emissions from commercial trucks [23]. With such substantial impacts from the freight transportation sector, the US federal government agencies have been taken the lead in emphasizing environmental sustainability. For example, the US Environmental Protection Agency (EPA) released the first federal standard for heavy-duty trucks in which specified a load-specific fuel consumption standard for medium- and heavy-duty trucks [24]. In addition, since freight transportation market is typically operated by private sectors, government is actively introducing incentives or financial support for eco-friendly logistics practices through several programs (e.g., Smart Way) [25]. Despite these efforts, most of the existing freight optimization models solely optimize operational efficiencies, such as transportation costs, travel time, or traffic volumes, without sufficient attentions on environmental measures.

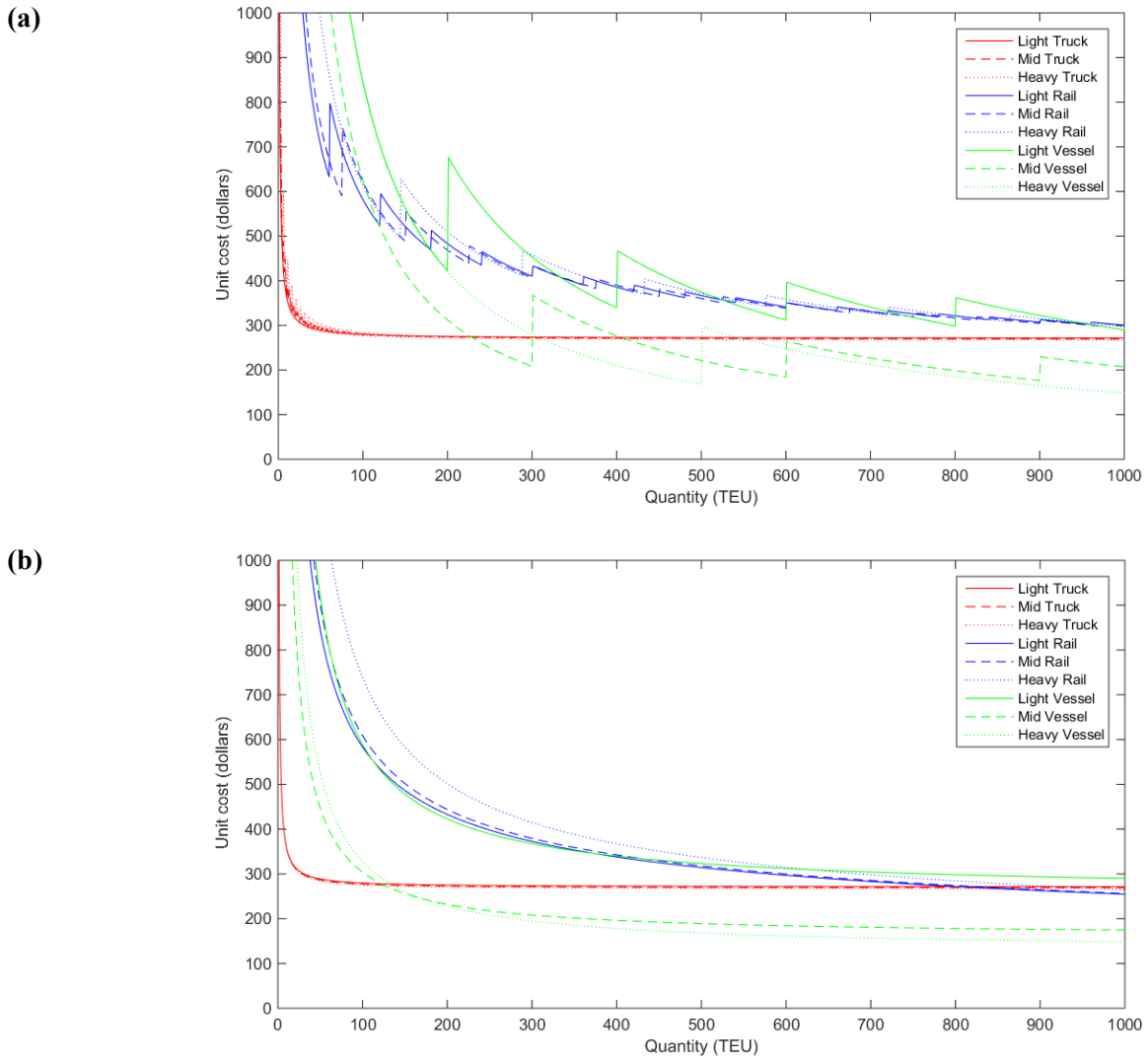

Figure 3: Unit cost curves (a) with economies of scale vs. (b) Smoothed fitted economies of scale

In summary, the body of the literature review revealed that the current state-of-the-practice on fleet dispatch tools need to be improved to comprehensively consider all factors of economies of scale. It was also revealed that current freight optimization tools need to be

upgrade for room for highlighting environmental impacts. In addition, the existing state-of-the-art tool do not ensure system optimal solution and is hard for practitioner to pick up. Therefore, it is needed to develop a multimodal freight optimization tool that is enhanced in the aforementioned aspects. The objective of this paper is to develop a multimodal fleet dispatching decision tool that has the following features:

- environmental cost is considered in addition to the transportation cost to support the environmentally conscious decisions;
- all three types of economies—economies of scale for quantity (EOQ), economies of scale for vehicle size (EOVS) and economies of scale for distance (EOD) —are incorporated;
- ensures system optimal dispatching solution;
- easy to use for practitioners

The rest of this section is organized as following: Problem Formulation section introduces the formulation of the MILP-based optimization tool. Model Evaluation section presents a case study and associated results. The Conclusions and Future Research section provides conclusion remarks and potential future research suggestions.

METHODOLOGY

The optimization problem was formulated as a Mixed Integer Linear Programming (MILP) model. Typically, a multimodal freight system comprises of hubs where cargos are stocked, distributed and/or transshipped among different freight modes. Thus the nodes in a typical network can be categorized as: *origin* (O_i)*, hub of origin* (h_o)*, hub of destination* (h_d), and *destination* (D_j). Thereby the links connecting two nodes can be grouped in four categories: *from origin* (O_i) *to hub of origin* (h_o), *from hub of origin* (h_o) *to hub of destination* (h_d), *from hub of destination* (h_d) *to destination* (D_j), and *from origin* (O_i) *to destination* (D_j). The decision variables and parameters for each of this category are assigned separately to appropriately incorporate the economies of scale into the MILP model. The detail efforts to realize the economies of scale under the MILP framework will be discussed later in this section. Remainder of this section explains the notations on the indices, parameters, decision variables, objective functions and constraints in detail.

The efforts of incorporating all three elements of the economies of scale (i.e., the economies of scale for quantity, the economies of scale for vehicle size, and the economies of scale distance) into a MILP scheme are described as follows:

- Economies of scale for quantity: The true economies of scale for quantity is incorporated into the model. It follows the pattern presented in Figure 3-(a), where unit cost shows instant jumps and no simplification is applied.
- Economies of scale for vehicle size: each vehicle size is assigned with its unique group of cost functions on various quantity levels. In other words, even for the same transport mode, different vehicle sizes are with different unit cost functions.
- Economies of scale for distance: Similar with the economies of scale for vehicle size, economies of scale for distance is incorporated by assigning unique unit distance transport cost to each link (i.e., from origin to hub of origin, from hub of origin to hub of destination, from hub of destination to destination, and from origin to destination).

Task 1: Formulation of Optimization Problem

Notation

The following lists the indices, parameters and variables utilized hereafter. The Twenty-foot Equivalent Unit (TEU) was used to describe the capacity of a cargo hereafter.

O_i Index for origin node, where $i \in I$

D_j Index for destination node, where $j \in J$

h_o Index for hub node at origin area, where $h_o \in H_O$

h_d Index for hub node at destination area, where $h_d \in H_D$

k Index for transporting mode system and vehicle size, where $k \in K = \{$light truck, mid truck, heavy truck, light rail, mid rail, heavy rail, light vessel, mid vessel, heavy vessel$\}$

$d_{m,n,k}$ Traveling distance from node m to node n using transporting mode k in km, where $m \in M = \{I, J, H_O, H_D\}, n \in N = \{I, J, H_O, H_D\}, k \in K$

$Ta_{i,ho,k}$ Transporting cost of haulage from origin i to hub at origin area h_o using transport mode k in $dollars / veh \cdot km$, where $i \in I$, $h_o \in H_O$ and $k \in K$

$Ea_{i,ho,k}$ Environmental cost of haulage from origin i to hub at origin area h_o using transport mode k in $dollars / veh \cdot km$, where $i \in I$, $h_o \in H_O$ and $k \in K$

$Tb_{ho,hd,k}$ Transporting cost of haulage from hub at origin area h_o to hub at destination area h_d using transport mode k in $dollars / veh \cdot km$, where $h_o \in H_O$, $h_d \in H_D$ and $k \in K$

$Eb_{ho,hd,k}$ Environmental cost of haulage from hub at origin area h_o to hub at destination area h_d using transport mode k in $dollars / veh \cdot km$, where $h_o \in H_O$, $h_d \in H_D$ and $k \in K$

$Tc_{hd,j,k}$ Transporting cost of haulage from hub at destination area h_d to destination node j using transport mode k in $dollars / veh \cdot km$, where $h_d \in H_D$, $j \in J$ and $k \in K$

$Ec_{hd,j,k}$ Environmental cost of haulage from hub at destination area h_d to destination node j using transport mode k in $dollars / veh \cdot km$, where $h_d \in H_D$, $j \in J$ and $k \in K$

$Td_{i,j,k}$ Transporting cost of haulage from origin i to destination j using transport mode k in $dollars / veh \cdot km$, where $i \in I$, $j \in J$ and $k \in K$

$Ed_{i,j,k}$ Environmental cost of haulage from origin i to destination j using transport mode k in $dollars / veh \cdot km$, where $i \in I$, $j \in J$ and $k \in K$

WI_i Terminal warehouse capacity at origin node i in TEU, where $i \in I$

WHo_{ho} Terminal warehouse capacity at hub at origin area h_o in TEU, where $h_o \in H_O$

WHd_{hd} Terminal warehouse capacity at hub at destination area h_d in TEU, where $h_d \in H_D$

WJ_j Terminal warehouse capacity at destination node j in TEU, where $j \in J$

D_j Demand at destination node j in TEU, where $j \in J$

R_k Available number of vehicles of transporting mode k, where $k \in K$

VS_k Capacity of individual vehicle of transporting mode k, where $k \in K$

Decision Variables

Decision variables are specified as follows. As shown below, this model comprises of the three types of decision variables: cargo quantities (i.e., X, Y, Z and V for each type of link category), binary variables which indicate whether arcs serve for any cargos (i.e., Xa, Ya, Za and Va for each type of link category) and number of vehicles associated with each link (i.e., Xb, Yb, Zb and Va for each type of link category).

$X_{i,ho,k}$ Cargo quantity from origin i to hub at origin area h_o using transport mode k, where $i \in I$, $h_o \in H_O$ and $k \in K$

$Y_{ho,hd,k}$ Cargo quantity from hub at origin area h_o to hub at destination area h_d using transport mode k, where $h_o \in H_O$, $h_d \in H_D$ and $k \in K$

$Z_{hd,j,k}$ Cargo quantity from hub at destination area h_d to destination node j using transport mode k, where $h_d \in H_D$, $j \in J$ and $k \in K$

$V_{i,j,k}$ Cargo quantity from origin i to destination j using transport mode k, where $i \in I$, $j \in J$ and $k \in K$

$Xa_{i,ho,k}$ If cargo is carried from origin i to hub at origin area h_o using transport mode k, then 1, otherwise 0, where $i \in I$, $h_o \in H_O$ and $k \in K$

$Ya_{ho,hd,k}$ If cargo is carried from hub at origin area h_o to hub at destination area h_d using transport mode k, then 1, otherwise 0, where $h_o \in H_O$, $h_d \in H_D$ and $k \in K$

$Za_{hd,j,k}$ If cargo is carried from hub at destination area h_d to destination node j using transport mode k, then 1, otherwise 0, where $h_d \in H_D$, $j \in J$ and $k \in K$

$Va_{i,j,k}$ If cargo is carried from origin i to destination j using transport mode k, then 1, otherwise 0, where $i \in I$, $j \in J$ and $k \in K$

$Xb_{i,ho,k}$ Number of vehicles of transport mode k served from origin i to hub at origin area h_o, where $i \in I$, $h_o \in H_O$ and $k \in K$

$Yb_{ho,hd,k}$ Number of vehicles of transport mode k served from hub at origin area h_o to hub at destination area h_d, where $h_o \in H_O$, $h_d \in H_D$ and $k \in K$

$Zb_{hd,j,k}$ Number of vehicles of transport mode k served from hub at destination area h_d to destination node j, where $h_d \in H_D$, $j \in J$ and $k \in K$

$Vb_{i,j,k}$ Number of vehicles of transport mode k served from origin i to destination j, where $i \in I$, $j \in J$ and $k \in K$

Objective Function

As aforementioned, the proposed MILP-based multimodal freight optimization model takes into account two types of costs (i.e., haulage costs and environmental cost). As shown in (11) the objective function is formulated in an additive form of four elements. Each element estimates the arc-specific total costs associated with the freight activities. For each element, the unit cost of haulage (e.g., Ta, Tb, Tc and Td) and environmental cost (e.g., Ea, Eb, Ec and Ed) per trip are augmented with the respective trip distance (d) and the number of vehicles which made the trips (e.g., Xb, Yb, Zb and Vb). It should be noted that the unit cost-parameters of haulage costs and the environmental costs are a function of cargo quantity (i.e., X, Y, Z and V for each type of link category) and trip distance.

$$\text{Min} \quad \sum_{i=1}^{I}\sum_{ho=1}^{HO}\sum_{k=1}^{K}(Ta_{i,ho,k}+Ea_{i,ho,k})\cdot d_{i,ho,k}\cdot Xb_{i,ho,k}+\sum_{ho=1}^{HO}\sum_{hd=1}^{HD}\sum_{k=1}^{K}(Tb_{ho,hd,k}+Eb_{ho,hd,k})\cdot d_{ho,hd,k}\cdot Yb_{ho,hd,k}+ \sum_{hd=1}^{HD}\sum_{j=1}^{J}\sum_{k=1}^{K}(Tc_{hd,j,k}+Ec_{hd,j,k})\cdot d_{hd,j,k}\cdot Zb_{hd,j,k}+\sum_{i=1}^{I}\sum_{j=1}^{J}\sum_{k=1}^{K}(Td_{i,j,k}+Ed_{i,j,k})\cdot d_{i,j,k}\cdot Vb_{i,j,k} \tag{11}$$

Unit Cost Functions Incorporating Economies of Scale

Unit cost estimation plays a key role in terms of cost optimization model. The proposed MILP-based freight optimization model adopted a set of unit cost functions which explicitly considered three types of economies scale. This research integrates the knowledge from literatures, the functions of unit cost of haulage for truck and rail system are borrowed from [12, 26] and the vessels unit cost of haulage is based on [10]. The estimation of environmental cost is adopted from [27] and [28]. The details of the unit cost functions adopted from these studies are found in the literatures [10, 12, 26-28]. The details of the unit cost functions adopted from these studies are shown in the Appendix.

Constraints

Constraint (12) and (13) specify the physical restrictions that the quantity of cargo outflow from a particular hub node should be less than or equal to the inflow of the corresponding hub node.

$$\sum_{i=1}^{I}\sum_{k=1}^{K}X_{i,ho,k}\geq\sum_{hd=1}^{HD}\sum_{k=1}^{K}Y_{ho,hd,k} \quad {}^{\forall}X_{i,ho,k}\in N,\ {}^{\forall}Y_{ho,hd,k}\in N \text{ where } N=\text{integer} \tag{12}$$

$$\sum_{ho=1}^{HO}\sum_{k=1}^{K}Y_{ho,hd,k}\geq\sum_{j=1}^{J}\sum_{k=1}^{K}Z_{hd,j,k} \quad {}^{\forall}Y_{ho,hd,k}\in N,\ {}^{\forall}Z_{hd,j,k}\in N \text{ where } N=\text{integer} \tag{13}$$

Constraint (14) through Constraint (17) specify that all cargos delivered to and from a particular node should not exceed the capacity of the terminal warehouse which is termed as WI_i, WHo_{ho}, WHd_{hd} and WJ_j for the origin, Hub of origin, Hub of destination, and destination, respectively.

$$\sum_{ho=1}^{HO}\sum_{k=1}^{K}X_{i,ho,k}+\sum_{j=1}^{J}\sum_{k=1}^{K}V_{i,j,k}\leq WI_i \quad {}^{\forall}X_{i,ho,k}\in N,\ {}^{\forall}V_{i,j,k}\in N \text{ where } N=\text{integer} \tag{14}$$

$$\sum_{i=1}^{I}\sum_{k=1}^{K}X_{i,ho,k}\leq WHo_{ho} \quad {}^{\forall}X_{i,ho,k}\in N \text{ where } N=\text{integer} \tag{15}$$

$$\sum_{ho=1}^{HO}\sum_{k=1}^{K} Y_{ho,hd,k} \le WHd_{hd} \quad {}^{\forall}Y_{ho,hd,k} \in N \text{ where } N = \text{integer} \tag{16}$$

$$\sum_{hd=1}^{HD}\sum_{k=1}^{K} Z_{hd,j,k} + \sum_{i=1}^{I}\sum_{k=1}^{K} V_{i,j,k} \le WJ_j \quad {}^{\forall}Z_{hd,j,k} \in N,\ {}^{\forall}V_{i,j,k} \in N \text{ where } N = \text{integer} \tag{17}$$

Constraint (18) states that the cargo delivered to each destination node should meet the demand of the destination node. The cargos can be reached to the destination nodes either through hubs ($Z_{hd,j,k}$) or through on-grounds option ($V_{i,j,k}$). Delivery of cargos more than the demand was allowed to make the optimization problem more flexible.

$$\sum_{hd=1}^{HD}\sum_{k=1}^{K} Z_{hd,j,k} + \sum_{i=1}^{I}\sum_{k=1}^{K} V_{i,j,k} \ge D_j \quad {}^{\forall}Z_{hd,j,k} \in N,\ {}^{\forall}V_{i,j,k} \in N \text{ where } N = \text{integer} \tag{18}$$

Constraint (19) through Constraint (21) state that the total vehicle used should not exceed the total number of available vehicles.

$$\sum_{k=1}^{3}\sum_{i=1}^{I}\sum_{ho=1}^{HO} Xb_{i,ho,k} + \sum_{k=1}^{3}\sum_{ho=1}^{HO}\sum_{hd=1}^{HD} Yb_{ho,hd,k} + \sum_{k=1}^{3}\sum_{hd=1}^{HD}\sum_{j=1}^{J} Zb_{hd,j,k} + \sum_{k=1}^{3}\sum_{i=1}^{I}\sum_{j=1}^{J} Vb_{i,j,k} \le R_{truck} \tag{19}$$
$${}^{\forall}Xb_{i,ho,k} \in N,\ {}^{\forall}Yb_{ho,hd,k} \in N,\ {}^{\forall}Zb_{hd,j,k} \in N,\ {}^{\forall}Vb_{i,j,k} \in N \text{ where } N = \text{integer}$$

$$\sum_{k=4}^{6}\sum_{i=1}^{I}\sum_{ho=1}^{HO} Xb_{i,ho,k} + \sum_{k=4}^{6}\sum_{ho=1}^{HO}\sum_{hd=1}^{HD} Yb_{ho,hd,k} + \sum_{k=4}^{6}\sum_{hd=1}^{HD}\sum_{j=1}^{J} Zb_{hd,j,k} + \sum_{k=4}^{6}\sum_{i=1}^{I}\sum_{j=1}^{J} Vb_{i,j,k} \le R_{rail} \tag{20}$$
$${}^{\forall}Xb_{i,ho,k} \in N,\ {}^{\forall}Yb_{ho,hd,k} \in N,\ {}^{\forall}Zb_{hd,j,k} \in N,\ {}^{\forall}Vb_{i,j,k} \in N \text{ where } N = \text{integer}$$

$$\sum_{k=7}^{9}\sum_{i=1}^{I}\sum_{ho=1}^{HO} Xb_{i,ho,k} + \sum_{k=7}^{9}\sum_{ho=1}^{HO}\sum_{hd=1}^{HD} Yb_{ho,hd,k} + \sum_{k=7}^{9}\sum_{hd=1}^{HD}\sum_{j=1}^{J} Zb_{hd,j,k} + \sum_{k=7}^{9}\sum_{i=1}^{I}\sum_{j=1}^{J} Vb_{i,j,k} \le R_{vessel} \tag{21}$$
$${}^{\forall}Xb_{i,ho,k} \in N,\ {}^{\forall}Yb_{ho,hd,k} \in N,\ {}^{\forall}Zb_{hd,j,k} \in N,\ {}^{\forall}Vb_{i,j,k} \in N \text{ where } N = \text{integer}$$

Constraint (22) through (29) entail that the number of vehicles used should match the quantity of cargo shipped.

$$X_{i,ho,k} > (Xb_{i,ho,k} - 1) \cdot VS_k + 1 \quad {}^{\forall}X_{i,ho,k} \in N,\ {}^{\forall}Xb_{i,ho,k} \in N \text{ where } N = \text{integer} \tag{22}$$

$$Y_{ho,hd,k} > (Yb_{ho,hd,k} - 1) \cdot VS_k + 1 \quad {}^{\forall}Y_{ho,hd,k} \in N,\ {}^{\forall}Yb_{ho,hd,k} \in N \text{ where } N = \text{integer} \tag{23}$$

$$Z_{hd,j,k} > (Zb_{hd,j,k} - 1) \cdot VS_k + 1 \quad {}^{\forall}Z_{hd,j,k} \in N,\ {}^{\forall}Zb_{hd,j,k} \in N \text{ where } N = \text{integer} \tag{24}$$

$$V_{i,j,k} > (Vb_{i,j,k} - 1) \cdot VS_k + 1 \quad {}^{\forall}V_{i,j,k} \in N,\ {}^{\forall}Vb_{i,j,k} \in N \text{ where } N = \text{integer} \tag{25}$$

$$X_{i,ho,k} \le Xb_{i,ho,k} \cdot VS_k \quad {}^{\forall}X_{i,ho,k} \in N,\ {}^{\forall}Xb_{i,ho,k} \in N \text{ where } N = \text{integer} \tag{26}$$

$$Y_{ho,hd,k} \le Yb_{ho,hd,k} \cdot VS_k \quad {}^{\forall}Y_{ho,hd,k} \in N,\ {}^{\forall}Yb_{ho,hd,k} \in N \text{ where } N = \text{integer} \tag{27}$$

$$Z_{hd,j,k} \le Zb_{hd,j,k} \cdot VS_k \quad {}^{\forall}Z_{hd,j,k} \in N,\ {}^{\forall}Zb_{hd,j,k} \in N \text{ where } N = \text{integer} \tag{28}$$

$$V_{i,j,k} \le Vb_{i,j,k} \cdot VS_k \quad {}^{\forall}V_{i,j,k} \in N,\ {}^{\forall}Vb_{i,j,k} \in N \text{ where } N = \text{integer} \tag{29}$$

Constraint (30) to Constraint (37) ensures that cargo shipped through each link matches its associated binary variable:

$$X_{i,ho,k} \le M \cdot Xa_{i,ho,k} \quad {}^{\forall}X_{i,ho,k} \in \mathbf{N},\ {}^{\forall}Xa_{i,ho,k} \in \{0,1\} \text{ where N} = \text{integer} \tag{30}$$

$$Y_{ho,hd,k} \le M \cdot Ya_{ho,hd,k} \quad {}^{\forall}Y_{ho,hd,k} \in \mathrm{N},\ {}^{\forall}Ya_{ho,hd,k} \in \{0,1\} \text{ where N = integer} \tag{31}$$

$$Z_{hd,j,k} \le M \cdot Za_{hd,j,k} \quad {}^{\forall}Z_{hd,j,k} \in \mathrm{N},\ {}^{\forall}Za_{hd,j,k} \in \{0,1\} \text{ where N = integer} \tag{32}$$

$$V_{i,j,k} \le M \cdot Va_{i,j,k} \quad {}^{\forall}V_{i,j,k} \in \mathrm{N},\ {}^{\forall}Va_{i,j,k} \in \{0,1\} \text{ where N = integer} \tag{33}$$

$$Xa_{i,ho,k} - X_{i,ho,k} \le 0 \quad {}^{\forall}X_{i,ho,k} \in \mathrm{N},\ {}^{\forall}Xa_{i,ho,k} \in \{0,1\} \text{ where N = integer} \tag{34}$$

$$Ya_{ho,hd,k} - Y_{ho,hd,k} \le 0 \quad {}^{\forall}Y_{ho,hd,k} \in \mathrm{N},\ {}^{\forall}Ya_{ho,hd,k} \in \{0,1\} \text{ where N = integer} \tag{35}$$

$$Za_{hd,j,k} - Z_{hd,j,k} \le 0 \quad {}^{\forall}Z_{hd,j,k} \in \mathrm{N},\ {}^{\forall}Za_{hd,j,k} \in \{0,1\} \text{ where N = integer} \tag{36}$$

$$Va_{i,j,k} - V_{i,j,k} \le 0 \quad {}^{\forall}V_{i,j,k} \in \mathrm{N},\ {}^{\forall}Va_{i,j,k} \in \{0,1\} \text{ where N = integer} \tag{37}$$

Task 2: Model Evaluation

To evaluate the performance of the proposed freight optimization model, the proposed model was compared against the two types of model: state-of-the-art model and a comparison model which was developed by combining the state-of-the-art model with an objective function considering the environmental costs [9-16]. Major features of the three models are described in the followings:

- *Proposed Model*: The proposed model incorporates all three economies of scale without simplification. As shown in Figure 3-(a), unit total cost estimations are discrete by different quantity, distance category and different vehicle types. The objective function both considers transportation cost and environmental cost.
- *State-of-the-art Model*: The state-of-the-art model considers all three economies of scale as well. However, it utilizes simplified smoothed fitted economies of scale as shown in Figure 3-(b) in the estimation of unit total cost. The objective function only considers transportation cost.
- *Comparison Model*: The comparison model also employs the simplified smoothed fitted economies of scale as featured by the state-of-the-art model. The objective function considers transportation cost and environmental cost as the same as the proposed model for a fair comparison.

Experimental Setup

As noted, a hypothetical multimodal network used for the case study is illustrated in Figure 4. The network comprised of six nodes: two Origin (Oi), two Destination (Dj), one Hub of origin (HO) and one Hub of destination (HD). Under this type of road network, cargos can be delivered through either truck-only freight option or intermodal freight option. The truck-only freight option represents a transport journey served only by trucks, and the intermodal freight option refers to a transport journey served by multiple transporting modes including truck, rail and vessel.

In this study, it was assumed that the cargos can be reserved in the hub unless they exceed the capacity of the warehouse facility. It implies that there is a possibility of transferring more cargos out of origin nodes than that arrive at the destination, thus some units of cargos can be left undelivered in the hub nodes as long as the demands at the destinations are met. Details on the case study settings are as follows:

- Maximum capacity of hub facility = 5,000 TEU
- Minimum demand at destination = 3,000 TEU
- Three types of vehicles are available: truck, rail and vessel
- Three levels of vehicle sizes are available for each vehicle type
- Available number of trucks for each vehicle size category = 700 vehicles

- Available number of rails for each different vehicle sizes = 30 vehicles
- Available number of vessels for each different vehicle sizes = 7 vehicles

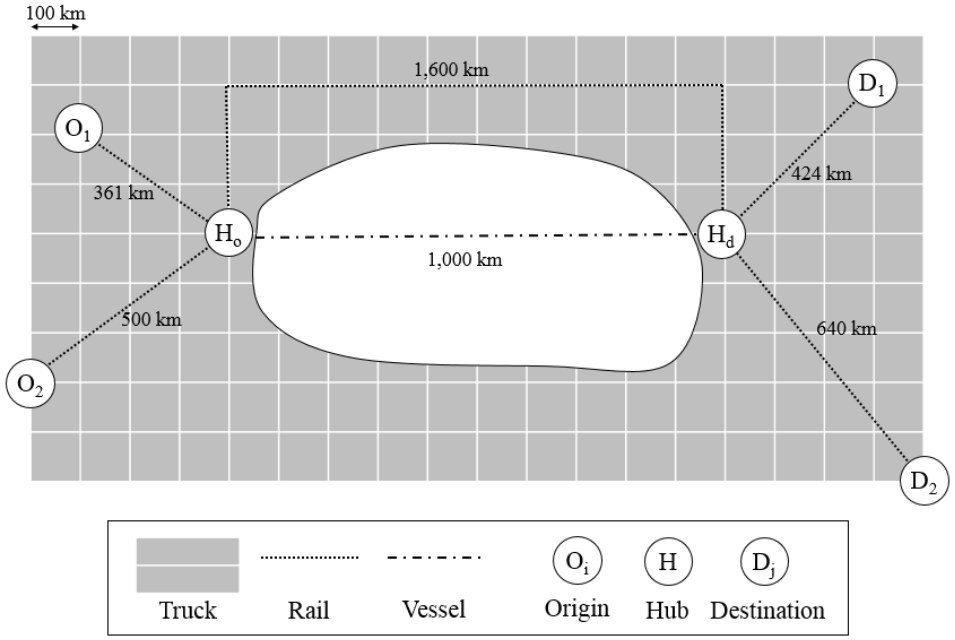

Figure 4: Network of multimodal freight system

All the proposed optimization formulation and the two models for comparisons were coded in the MATLAB [29] and the intlinprog solver were used to find the solution resulting in the minimum total costs subject to integer constraints. The key parameters of the intlinprog solver chosen for this research are summarized in Table 2.

Table 2: Parameters of intlinprog Solver

Parameter	Description and Features	Value
AbsoluteGapTolerance (i.e., Stopping criterion)	Solver stops if the difference between the internally calculated upper and lower bounds on the objective function is less than or equal to this value (subject to nonnegative real number)	0
BranchRule	Rule for choosing the component for branching	Maxpscost (i.e., Branch-and-bound)
ConstraintTolerance	The maximum discrepancy that linear constraints can have and still be considered satisfied. The available range of the parameter is between 10-9 and 10-3	10-4
CutGeneration	Level of cut generation	Basic (i.e., Normal cut generation)
CutMaxIterations	Number of passes through all cut generation methods before entering the branch-and-bound phase. The available range of the parameter is	10

	between 1 through 50.	

RESULTS AND ANALYSIS

As shown in Table 3, the results demonstrate that the proposed model is significantly different from both of the state-of-the-art model and the comparison model. The results show that the state-of-the-art and the comparison model inclined to utilize the truck-only freight scheme over the intermodal freight scheme in their optimal strategy, while the proposed model takes more advantage of the Intermodal freight scheme. In addition, the proposed model produced the fair distributions of cargos among different vehicle sizes, while the comparison model assigned cargos with preference to relatively heavier-sized vehicles. This results clearly show one of the challenges of not considering the economies of scale in a proper way for the comparison model; the comparison model merely takes advantage of the low unit costs associated with the heavier-sized vehicles as it was demonstrated in Figure 3-(b), but the optimization model ignores the effect of having additional vehicles on the unit costs that results in the fluctuations in the unit costs as in Figure 3-(a). Table 4 shows the comparison of the total costs between the proposed model and the two models compared. The proposed model saves cost by 6.3 % over the comparison model and by 21.3% over the state-of-the-art model.

Table 3 Comparisons of Optimal Strategies between the State-of-the-art Model vs. the Comparison Model vs. Proposed Model

State-of-the-art Model

(Origin-Destination)	Light Truck	Mid Truck	Heavy Truck	Light Rail	Mid Rail	Heavy Rail	Light Vessel	Mid Vessel	Heavy Vessel
O1 - D1	4	0	0	N/A	N/A	N/A	N/A	N/A	N/A
O1 - D2	0	0	0	N/A	N/A	N/A	N/A	N/A	N/A
O2 - D1	0	0	0	N/A	N/A	N/A	N/A	N/A	N/A
O2 - D2	696	0	0	N/A	N/A	N/A	N/A	N/A	N/A
O1 - Ho	0	1376	830	1740	1050	0	N/A	N/A	N/A
O2 - Ho	0	16	0	0	0	288	N/A	N/A	N/A
Ho - Hd	0	0	0	0	0	0	0	1800	3500
Hd - D1	0	8	0	60	1200	1728	N/A	N/A	N/A
Hd - D2	0	0	0	0	0	2304	N/A	N/A	N/A

Comparison Model

(Origin-Destination)	Light Truck	Mid Truck	Heavy Truck	Light Rail	Mid Rail	Heavy Rail	Light Vessel	Mid Vessel	Heavy Vessel
O1 - D1	4	0	0	N/A	N/A	N/A	N/A	N/A	N/A

O1 - D2	0	0	0	N/A	N/A	N/A	N/A	N/A	N/A
O2 - D1	0	0	0	N/A	N/A	N/A	N/A	N/A	N/A
O2 - D2	696	0	0	N/A	N/A	N/A	N/A	N/A	N/A
O1 - Ho	0	1392	829	1800	975	0	N/A	N/A	N/A
O2 - Ho	0	4	0	0	300	0	N/A	N/A	N/A
Ho - Hd	0	0	0	0	0	0	0	1800	3500
Hd - D1	0	4	1	0	975	2016	N/A	N/A	N/A
Hd - D2	0	0	0	0	0	2304	N/A	N/A	N/A

Proposed Model

(Origin-Destination)	Light Truck	Mid Truck	Heavy Truck	Light Rail	Mid Rail	Heavy Rail	Light Vessel	Mid Vessel	Heavy Vessel
O1 - D1	0	0	0	N/A	N/A	N/A	N/A	N/A	N/A
O1 - D2	0	0	0	N/A	N/A	N/A	N/A	N/A	N/A
O2 - D1	0	0	0	N/A	N/A	N/A	N/A	N/A	N/A
O2 - D2	50	0	0	N/A	N/A	N/A	N/A	N/A	N/A
O1 - Ho	620	1398	1482	1500	0	0	N/A	N/A	N/A
O2 - Ho	11	0	0	0	75	864	N/A	N/A	N/A
Ho - Hd	0	0	0	0	0	0	0	2450	3500
Hd - D1	9	0	0	240	2175	576	N/A	N/A	N/A
Hd - D2	10	0	0	60	0	2880	N/A	N/A	N/A

Table 4: Total Cost Comparison

Model Type	Total Cost (in dollars)
State-of-the-art Model	$ 302,008,000
Comparison Model	$ 253,841,000
Proposed Model	$ 237,785,000

Sensitivity analysis on varying demands was conducted for the proposed model in terms of total cost, transportation cost and environmental cost. As shown in Figure 5, the proposed

model generally outperforms the both of the comparison model and state-of-the-art model and saves cost by up to 6.3% over the comparison model and 21.3% over the state-of-the-art model.

The results of the state-of-the-art model are intuitive that it shows higher total costs as the objective function of the model did not consider the environmental costs. The results of the comparison model are also explanatory that the difference between the proposed model and the comparison model is whether or not considering the discrete increment of unit cost according to the batch strategies. No benefit could be gained by applying the proposed model in case where the cargo quantity equals to the capacity of the vehicle fleet picked, while the benefit from the proposed model over the comparison model becomes maximized when a new vehicle fleet is just added which is partially filled with small cargo quantity.

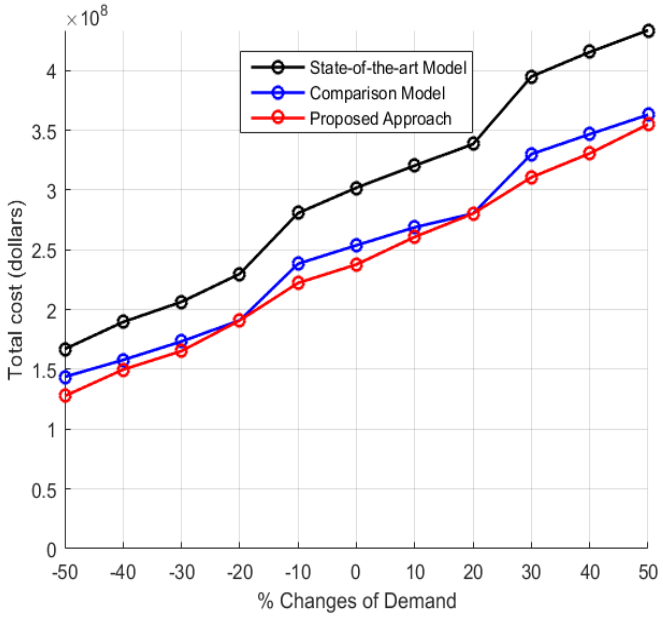

Figure 5: Sensitivity study on demand

The proposed model was further investigated by breaking down the total cost into transportation cost and environmental cost. As shown in Figure 6, no adverse effect was caused by the proposed model with respect to the various demands. Depending on the cargo demands, the savings varied, but the proposed model benefit both the transportation cost and environmental cost. When the proposed model was compared with the comparison model, the savings in transportation cost was up to 6.9% at the demand of 3,900 TEU (+30% of the base case) and the savings in environmental cost was up to 17.1% at the demands of 2,700 TEU (-10% of the base case). When it was compared with the state-of-the-art model, the savings in transportation cost was up to 15.1% at the demand of 3,000 TEU (the base case) and the savings in environmental cost was up to 61.4% at the demands of 2,400 TEU (-20% of the base case).

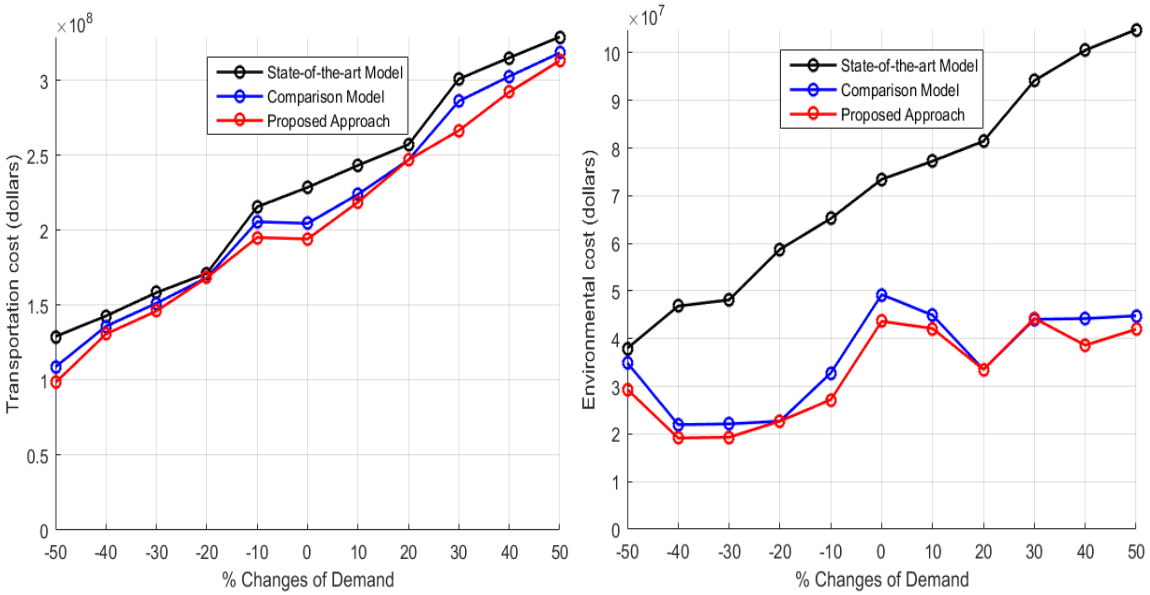

Figure 6: Breakdown into transportation cost and environmental cost

CONCLUSIONS & RECOMMENDATIONS

A multimodal freight dispatching tool is proposed. The highlights of this new dispatching tool include that (i) environmental costs is considered in addition to the transportation cost to support the environmentally conscious decisions; (ii) all three types of economies — economies of scale for quantity (EOQ), economies of scale for vehicle size (EOVS) and economies of scale for distance (EOD) — are incorporated; (iii) ensures system optimal dispatching solution; (iv) easy to use for practitioners. The proposed model was evaluated in terms of total cost, transportation cost and environmental cost. Sensitivity analysis was conducted with regard to various demands, and the results prove that the proposed model outperforms both the state-of-the-art model and the comparison model which combines the state-of-the-art model with environmental consideration. The proposed model saves cost up to 6.3% over the comparison model and up to 21.3% over the state-of-the-art model, which varies based on demand. Detailed investigation revealed that the proposed model has no adverse effect on both transportation cost and environmental cost.

Although the proposed fleet dispatching tool successfully showed its robustness as well as significant benefit, the current proposed model could only provide suggestions when cargo demand does not exceed capacity. Future research could consider strengthening the dispatching model by enabling the capability of determining number of extra vehicle needed when capacity is insufficient.

III. FUEL CONSUMPTION AND EMISSIONS MODEL FOR HEAVY DUTY DIESEL TRUCKS: MODEL DEVELOPMENT AND TESTING

PROBLEM STATEMENT

Transportation activities account for 28% of the total U.S. energy use and 33.4% of carbon dioxide (CO_2, the major component of greenhouse gas (GHG) emissions) production [30, 31]. Consequently, numerous efforts are being tested in an attempt to reduce transportation-related energy consumption and GHG emissions with the incremental intensification of the global energy crisis and negative GHG effects. Furthermore, the energy use also results in severe air pollution (e.g. Hydrocarbon HC, Carbon Monoxide CO, Nitric Oxide NOx), significantly deteriorating air quality and dwelling environment. As the majority of vehicle fleet, passenger cars have attracted significant attention in the past decade, and reduction in fuel consumption and emission levels have been achieved through the development of relevant regulations and technical solutions. As a counterpart, however, the investigation of heavy duty diesel truck (HDDT) fuel consumption behavior is relatively less mature compared to that of gasoline passenger cars. Although HDDTs make up only a fraction of the total vehicle population, they are major contributors to GHG emissions and air pollutants, accounting for 22.8% of the total CO_2 production [31] and 50% of NOx emissions [32] in the transportation sector.

HDDTs are receiving increasing attention from legislators, the government and society at large. For example, in September 2011, the National Highway Traffic Safety Administration (NHTSA) and the U.S. Environmental Protection Agency (EPA) jointly promulgated the first-ever federal regulations mandating improvements in fuel economy of heavy-duty commercial vehicles [33]. Furthermore, researchers have been committed to developing road eco-freight strategies [34-37] in order to support "green transportation" policy making.

Accurate and efficient models are needed to provide robust estimates in support of quantifying potential reductions in fuel consumption and emission levels induced by implementing eco-friendly strategies, such as developing eco-routing [38-40] or eco-driving systems [41-45] and utilizing advanced fuel techniques [46-48] or alternative fuels [49-52]. Among the existing modeling efforts, most are operated at a macroscopic or microscopic level. The macroscopic models, such as MOBILE 6.2 [53], were demonstrated to produce unreliable estimates due to their inability of capturing transient vehicle activities [54]. Consequently, they are incapable of being utilized for the energy and environmental assessment of traffic operational projects. Microscopic models were introduced in order to better capture the variability associated with vehicle dynamics. A wide range of instantaneous models have been developed using in-laboratory or field data, and some of them are applicable to modeling HDDTs, such as MOVES, VT-Micro [55], the Passenger Car and Heavy Duty Emission Model (PHEM) [56], VERSIT [57], the Comprehensive Modal Emissions Model (CMEM) [58, 59].

The majority of the aforementioned models, however, have limitations in use. For example, MOVES, which was developed as an inventory model based on a wide range of data sources, is capable of providing robust estimates. Nonetheless, it requires massive user inputs for each run, which significantly increases the time required to run multiple scenarios and large networks. CMEM generally underestimates fuel consumption levels for acceleration maneuvers; more importantly, it characterizes fuel consumption as a linear function of vehicle power, which produces a bang-bang type of control system. A bang-bang control may arise when the partial derivative of the response with respect to the control variable is not a function of the control variable (a more detailed description of a bang-bang control system is provided in subsequent sections. The fuel estimate module for CMEM is addressed in (38):

$$\mathrm{FR} = \frac{K \times N \times V + \frac{P}{\eta}}{43.2} \times [1 + b_1 \times (\mathrm{N} - \mathrm{N}_0)^2] \quad (38)$$

Here FR is the fuel rate in g/s, K is the engine friction factor, N is engine speed in (revolutions per second), V is engine displacement in liters, η is the efficiency for diesel engines, b1 equals to $1\mathrm{E}-04$, N_0 is a constant related to engine displacement, 43.2 KJ/g is the lower heating value of a typical diesel fuel, and P is the vehicle power which is the control variable of the fuel model. Since the fuel rate is affine to the vehicle power, its partial derivative with respect to power is independent of the power. This results in the minimum fuel consumption levels being achieved only at the point of Pmin or P_{max}, which implies that a vehicle should be in "full throttle/full braking" to capture optimal events. Another limitation of CMEM is that it cannot be easily calibrated without engine data (e.g. engine speed), which increases the difficulty for its efficient use in simulation systems. Like CMEM, PHEM and VERSIT also produce a bang-bang control. VT-Micro is capable of circumventing the bang-bang control; however, it requires a large amount of in-laboratory or field data to be calibrated, which is cost-prohibitive and time-consuming.

RESEARCH OBJECTIVE AND APPROACH

Overall, the existing models either produce a bang-bang type of control system or cannot be easily calibrated or efficiently used. Consequently, a simple, accurate and efficient model is needed. Rakha et al. [60] developed the Virginia Tech Comprehensive Power-based Fuel consumption Modeling (VT-CPFM) framework by characterizing fuel consumption levels as a second-order polynomial function of vehicle power to circumvent the bang-bang control problem. Furthermore, the model offers a unique ability to be calibrated using publicly available data (a more detailed description of the calibration procedure is provided in [60]) without massive data collection. Recent efforts have validated the applicability of the model for light duty vehicles (LDVs) [61] and transit buses [62, 63] under real-world driving conditions; however, it has not been expanded to HDDTs yet. Consequently, the study is intended to develop the VT-CPFM-based fuel consumption and emission model for HDDTs in order to circumvent the bang-bang problem in the modeling practice. The developed model will support to design eco-routing and eco-driving systems in future studies.

METHODOLOGY

The HDDT model is developed using a framework which is very similar to that of other models within the VT-CPFM program. As a power-based model, the VT-CPFM framework uses a bottom-up approach. Namely, the parameters, such as resistance force, used for power estimation are first computed by a resistance force module; and thereafter the vehicle power is estimated with an engine power module which characterizes the vehicle power as a function of the resistance forces. The fuel consumption is then estimated using a fuel rate module that models the fuel consumption as a polynomial function of the vehicle power. Finally, the emissions for HC, CO, NOx were mathematically characterized as a function of fuel consumption and speed.

Model Structure

Resistance Force Module

The resistance force is computed considering a combination of aerodynamic, rolling, and grade resistance forces, as expressed in (39):

$$\mathrm{R(t)} = \frac{\rho}{25.92} C_d C_h A_f v(t)^2 + 9.8066m\frac{C_r}{1000}(c_1 v(t) + c_2) + 9.8066mG(t) \quad (39)$$

where R(t) is the vehicle resistance force (N); ρ is the air density at sea level at a temperature of 15 ℃(59 °F) (equal to 1.2256 $\mathrm{kg/m^3}$); C_d is the drag coefficient (unitless) which is determined by truck type, 0.78 is used for the tested trucks (no aerodynamic aids) in this study [64]; C_h is the correction factor for altitude (unitless), calculated by 1-0.085H (H is the altitude in km); A_f is the frontal area of trucks ($\mathrm{m^2}$), 10.7 $\mathrm{m^2}$ is used based on the truck type; v(t) is the velocity in km/h; m is the vehicle mass in kg; Cr, c1 and c2 are the rolling resistance parameters (unitless), which vary as a function of road surface type and conditions as well as vehicle tire type; their typical values could be obtained from [64, 65]. $G(t)$ is the instantaneous road grade which is determined by elevation profiles.

Vehicle Power Module

The power exerted at any instant t is formulated by [66] as expressed in (40):

$$\mathrm{P(t)} = \frac{R(t) + (1 + \lambda + 0.0025\xi v(t)^2)ma(t)}{3600\eta} v(t) \quad (40)$$

where P(t) is the vehicle power in kW; λ is the mass factor accounting for rotational masses, a value of 0.1 is used for heavy duty vehicles (HDVs) [67, 68]; ξ is the gear ratio and assumed to be zero in this paper due to the lack of engine gear data. $a(t)$ is the instantaneous acceleration (m/s^2); η is the driveline efficiency.

Fuel Consumption Module

As illustrated in Figure 7, HDDTs present similar fuel consumption behavior compared to transit buses as seen in Wang and Rakha [62] with the fuel consumption rate a concave function of vehicle power for the positive power condition, and almost constant for the negative condition. Consequently, the general structure of the model has been specified as a two-regime mechanism. Rakha et al. [60] developed two VT-CPFM frameworks (VT-CPFM-1 and VT-CPFM-2) for LDVs each of which is a two-regime model and characterizes fuel consumption as a second-order polynomial function of vehicle power. The use of a second order model ensures that a bang-bang control does not result from the application of the model. Furthermore, the model higher than second-order may not be calibrated using standard drive cycles given the complexity of the higher order model. Consequently, a second-order model achieves a good trade-off between model accuracy and applicability. Only VT-CPFM-1 is utilized to develop the model in this study given that VT-CPFM-2 requires additional gear data which is typically not available. The VT-CPFM-1 framework is expressed in (41):

$$\mathrm{FC} = \begin{cases} \alpha_0 + \alpha_1 P(t) + \alpha_2 P(t)^2, & \forall P(t) \geq 0 \\ \alpha_0\,, & \forall P(t) < 0 \end{cases} \quad (41)$$

Here FC (t) is the fuel consumption rate at instant t [l/s]; α_0, α_1 and α_2 are the vehicle specific model coefficients that remain to be calibrated.

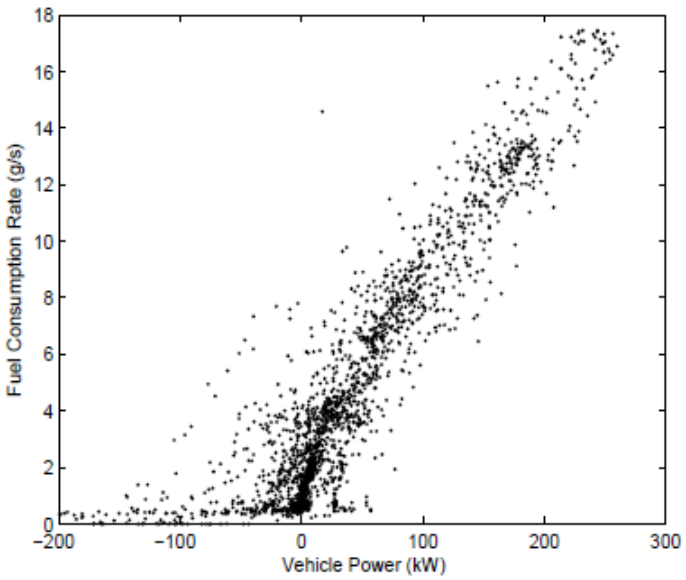

Figure 7: Vehicle power vs. Truck fuel consumption functional form

It should be noted that the model coefficients, α_0, α_1, and α_2, could be calibrated using publicly available data using (42), (43), and (44):

$$\alpha_0 = \frac{P_{fmp}\omega_{idle}d}{22164(HV)N} \tag{42}$$

$$\alpha_2 = \frac{\left(F_{city} - F_{hwy}\frac{P_{city}}{P_{hwy}}\right) - \left(T_{city} - T_{hwy}\frac{P_{city}}{P_{hwy}}\right)\alpha_0}{P_{city}^2 - P_{hwy}^2\frac{P_{city}}{P_{hwy}}} \tag{43}$$

$$\alpha_1 = \frac{F_{hwy} - T_{hwy}\alpha_0 - P_{hwy}^2\alpha_2}{P_{hwy}} \tag{44}$$

Here P_{fmp} is the idling fuel mean pressure (400,000 Pa); d is the engine displacement (liters); HV is the fuel lower heating value (43,200,000 J/kg for conventional diesel fuel); N is the number of engine cylinders; ω_{idle} is the engine idling speed (rpm); F_{city} and F_{hwy} (liters) are the fuel consumed for the EPA city and highway drive cycles; P_{city}, P_{city}^2, P_{hwy}, P_{hwy}^2 are the sum of the power and power squared over the EPA city- and highway cycle respectively; T_{city} and T_{hwy} are the duration of EPA city and highway drive cycles (s). Most of the parameters typically correspond to either physical characteristics of the vehicles or fuel type, so that they are stated as specifications by the vehicle manufacturers and readily available.

Nonetheless, the fuel economy, used to estimate F_{city} and F_{hwy}, cannot be obtained in this study given that HDDTs do not report their fuel economy for standard drive cycles (e.g. the EPA highway and city drive cycles). Consequently, the HDDT model, unlike LDVs, currently cannot be developed using publicly available data; instead, real-world data were gathered.

Emissions Module

The VT-CPFM model was extended to modeling HC, CO, NOx emissions based on the estimated fuel consumption levels. Different model specifications were tested to determine which parameters would be used in the emission model. Stepwise regression analysis was used

to determine the mathematical functionality. The final emission modeling framework is illustrated in (45), in which the square root of the emission is characterized as a polynomial function of speed and fuel consumption, and a, b, c, d, e, f, g, h are model parameters to be calibrated. The square root model guarantees that the emission results will always be positive.

$$\sqrt{E(t)} = a + b.v(t) + c.F(t) + d.v(t).F(t) + e.F(t)^2 + f.F(t)^3 + g.v(t).F(t)^2 + h.v(t).F(t)^3 \quad (45)$$

Data Preparation

The data used for model development were collected and provided by the researchers at University of California (UC) at Riverside.

Vehicle Recruitment

The modeling effort is aimed to test the applicability of the VT-CPFM framework to modeling the HDDTs within diverse vehicle-technology categories. Consequently, the recruited trucks should differ in a wide range of vehicle-specific parameters. To this end, a total of eight trucks were randomly recruited from used vehicle fleets in Southern California within test categories by vehicle model year and engine model/displacement, and a balance between horse power and manufacturers was attempted. The detailed vehicle information is presented in Table 5. For simplicity, the eight vehicles, from the top to the bottom of Table 5**Error! Reference source not found.** are labeled as HDDT1, HDDT2, HDDT3, HDDT4, HDDT5, HDDT6, HDDT7, and HDDT8 respectively in the following sections.

Table 5: Vehicle Information

Make/Model	Model Year	Engine Make/Model	Rated Power (hp)	Engine Size (l)	Vehicle Mass (kg)
International/ 9800 SBA	1997	Cummins/M11-330	330	10.8	7182
Freightliner/ D120	1997	DDC/C-60	360/400	12.7	7758
Freightliner/ D120	1997	Cummins/N14	370/435	14	7029
Freightliner/ C-120	1997	Cummins/N14	370/435	14	7623
Freightliner/ C-120	1998	DDC/C-60	370/430	12.7	8028
Freightliner/ FDL 120	1999	DDC/C-60	470	12.7	8118
Freightliner/ FDL 120	1999	DDC/C-60	360	12.7	8118
Freightliner/FLD 120	2001	CAT/C-15	475	14.6	7092

Data Set

Given that in-laboratory data (i.e. chassis dynamometer testing) are not always reflective of real-world driving conditions, on-road data were gathered instead.

To measure real-world fuel consumption and emission levels more realistically, UC Riverside developed a mobile emissions research laboratory (MERL) that contains all instrumentation that is normally found in a regular vehicle emission laboratory. MERL weighs approximately 45,000 lbs. and could serve as a truck load, so that it is capable of capturing the transient fuel consumption and emissions of a truck pulling it when the truck is being tested. Further details of MERL can be found in [59, 69].

The HDDT test was conducted, by the Center for Environmental Research and Technology at UC Riverside, on the roadways in California's Coachella Valley involving long, uninterrupted stretches of road, approximately at sea level. All trucks were tested using standard fuel from the same source. The data were recorded at a frequency of 1 Hz and a total of 238,893 seconds of data were gathered with a collection of 8 parameters for each truck, including CO2,

Carbon Monoxide (CO), and Hydro Carbon (HC), Oxides of Nitrogen (NOx), velocity, fuel rate, engine speed and elevation. For more details on data collection procedure, the reader is encouraged to read Barth, et al. [59].

Data Post-processing

The raw fuel consumption rates were in g/s and then converted to l/s in order to use the VT-CPFM framework to develop the proposed model. Simultaneously, the unit of velocity was converted from mi/h to km/h for modeling purposes.

Through comparing the second-by-second emissions with engine control unit (ECU) data (i.e. velocity, fuel rate and engine speed), a time delay was found to exist. Consequently, a time alignment was needed to synchronize the raw data. Since fuel rates have a strong relationship with emissions, they were utilized to determine the value of the required time shift. The proper time shift was determined through a cross-correlation analysis by which the correlation coefficients between emissions and fuel rates were estimated by a correlation function for a range of lag times. The lag times with the highest correlations were selected as the optimal events. It should be noted that the emission data for some of the testing trucks (CO_2 collected by HDDT 4 and HDDT 5, CO by HDDT 4, and HC by HDDT 7) are invalid due to an error in the emission sensors of MERL during data collection, and thus the model does not cover these vehicles.

The aligned data was smoothed by a moving average filter, and outliers were identified using a cook's distance procedure.

RESEARCH FINDINGS

The modeling results are presented for fuel consumption and emission respectively in this section.

Fuel Consumption Model Development

Each tested truck was individually modeled. Table 6 gives a generalization of the model inputs along with their sources. Some of the variables are capable of being gathered in the field (e.g. vehicle speed), and some can be obtained from either the literature or manufacturer websites (e.g. drag coefficient, vehicle mass).

Table 6: Parameters required for model calibration

Parameter	Value	Source
Drag coefficient (C_d)	0.78	[64]
Altitude correction factor (C_h)	N/Aa	Computed from field data
Vehicle frontal area (A_f)	10.0 m^2	[64]
Vehicle speed (v)	N/A[a]	Measured in field
Mass (m)	N/A[a]	Measured in field
Rolling coefficient (C_r)	1.25	[64]
c_1	0.0328	[64]
c_2	4.575	[64]
Road grade(G)	N/A[a]	Computed from field data
Acceleration (a)	N/A[a]	Computed from field data
Driveline efficiency (η)	0.94	[64]

[a]The parameter is not a single value.

Fuel Consumption Model Calibration Challenges

The model was calibrated using general linear regression analysis, and model coefficients are summarized in Table 7. Unlike LDVs, the second-order parameters(α_2) are negative, which

demonstrates that fuel consumption varies as a concave polynomial function of vehicle power and exhibits a mild growth when vehicle power is increasing. This is similar to transit buses in [62, 63] in which the concave model was demonstrated to accurately predict fuel consumption levels.

Table 7: The concave model for each truck

Truck classification	α_0	α_1	α_2
HDDT 1	1.13E-03	1.11E-04	-1.71E-07
HDDT 2	1.88E-03	1.01E-04	-1.27E-07
HDDT 3	1.56E-03	1.09E-04	-1.24E-07
HDDT 4	1.42E-03	1.03E-04	-1.22E-07
HDDT 5	1.38E-03	1.10E-04	-1.64E-07
HDDT 6	1.02E-03	1.06E-04	-9.28E-08
HDDT 7	9.18E-04	1.06E-04	-8.75E-08
HDDT 8	2.02E-03	8.78E-05	-3.33E-08

Nonetheless, the concave model may produce unrealistic driving recommendations as demonstrated by the sensitivity of estimated optimum fuel economy cruise speed to road grade and vehicle weight, as illustrated in Figure 8 and Figure 9, respectively. The road grade varies from -8% to 8% with a span of 2%, and the vehicle weight varies from 17,000 kg to 38,000 kg by having an identical span of 1000 kg. Figure 8 characterizes the variation of fuel consumption levels over cruise speed at different grade levels, which produces counter intuitive fuel consumption levels, especially when the road grade is high. This implies that the optimum fuel economy cruise speed may increase with the rise of road grade. Figure 9 also gives unrealistic results that heavier vehicles have higher optimum cruise speeds, implying that, drivers of heavier vehicles, compared to those driving lighter vehicles, are recommended to achieve higher cruise speed to minimize their fuel consumption levels. This is obviously not correct in reality.

Given that the concave model generates a mild increase of fuel consumption with the growth of vehicle power, the unrealistic driving recommendations cannot be avoidable.

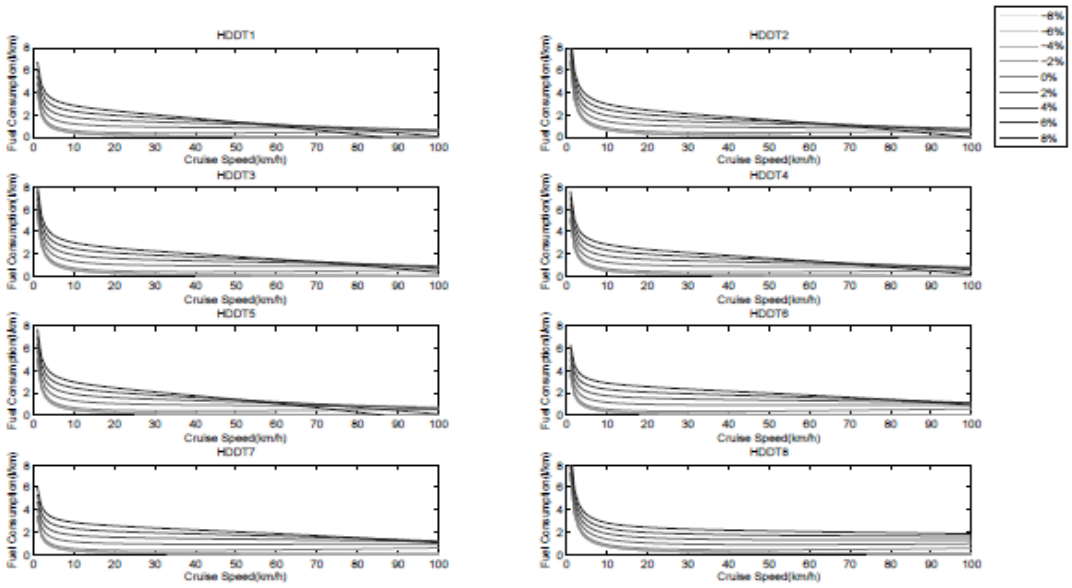

Figure 8: Fuel consumption levels vs. cruise speed at different grade levels (concave model)

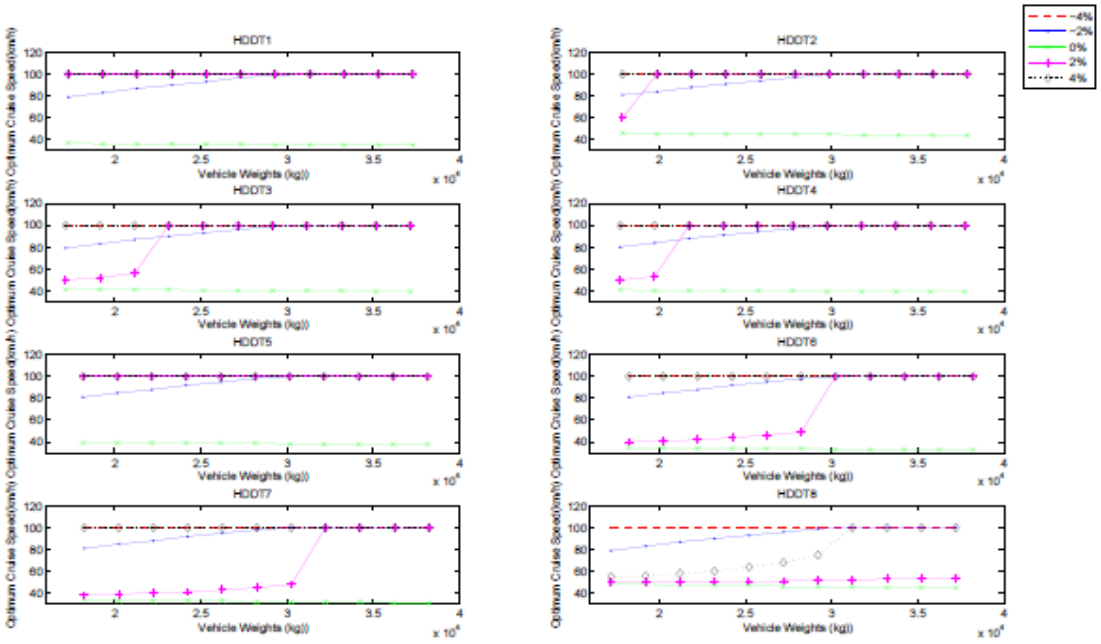

Figure 9: Impacts of vehicle weight on the optimum fuel economy cruise speed at different grade levels (concave model)

Fuel Consumption Model Enhancement

Given the deficiency of the concave model, an enhancement was considered to make the model more realistic. The convex model had been developed for LDVs and validated to be capable of generating reasonable driving instructions in existing eco-driving and eco-routing [40, 41, 70]. Consequently, the model was alternatively developed by ensuring that the second-order parameter is positive (linear model has not been considered given that it produces a bang-bang control).

To develop a convex model, the order of magnitude of the second-order parameter, which impacts the degree of convexity of the function, needs to be determined. Basically, a lower order of magnitude generates estimates of the convex model less consistent with those of the concave model. Nonetheless, a higher order of magnitude, although more accurate, is very similar to a linear model. A trade-off is thus needed between the accuracy of the model and the degree of convexity. The performance of the convex model in terms of R^2 values has been comprehensively investigated by varying the order of magnitude from $1E-05$ to $1E-11$, as illustrated in Figure 10. For each model, the R-square value increases with the growth of the order of magnitude, while the performance achieves little improvement when the coefficient is higher than$1E-08$. Consequently, $1E-08$ was considered as the best order of magnitude in balancing the model performance and the degree of convexity of the model. Convex model is summarized in Table 8.

Table 8: The convex model for each truck

Truck classification	α_0	α_1	α_2
HDDT 1	1.56E-03	8.10E-05	1.00E-08
HDDT 2	2.48E-03	7.14E-05	1.00E-08
HDDT 3	2.26E-03	7.82E-05	1.00E-08
HDDT 4	1.80E-03	7.96E-05	1.00E-08
HDDT 5	2.02E-03	7.59E-05	1.00E-08
HDDT 6	1.45E-03	8.48E-05	1.00E-08

HDDT 7	1.31E-03	8.63E-05	1.00E-08
HDDT 8	2.16E-03	7.98E-05	1.00E-08

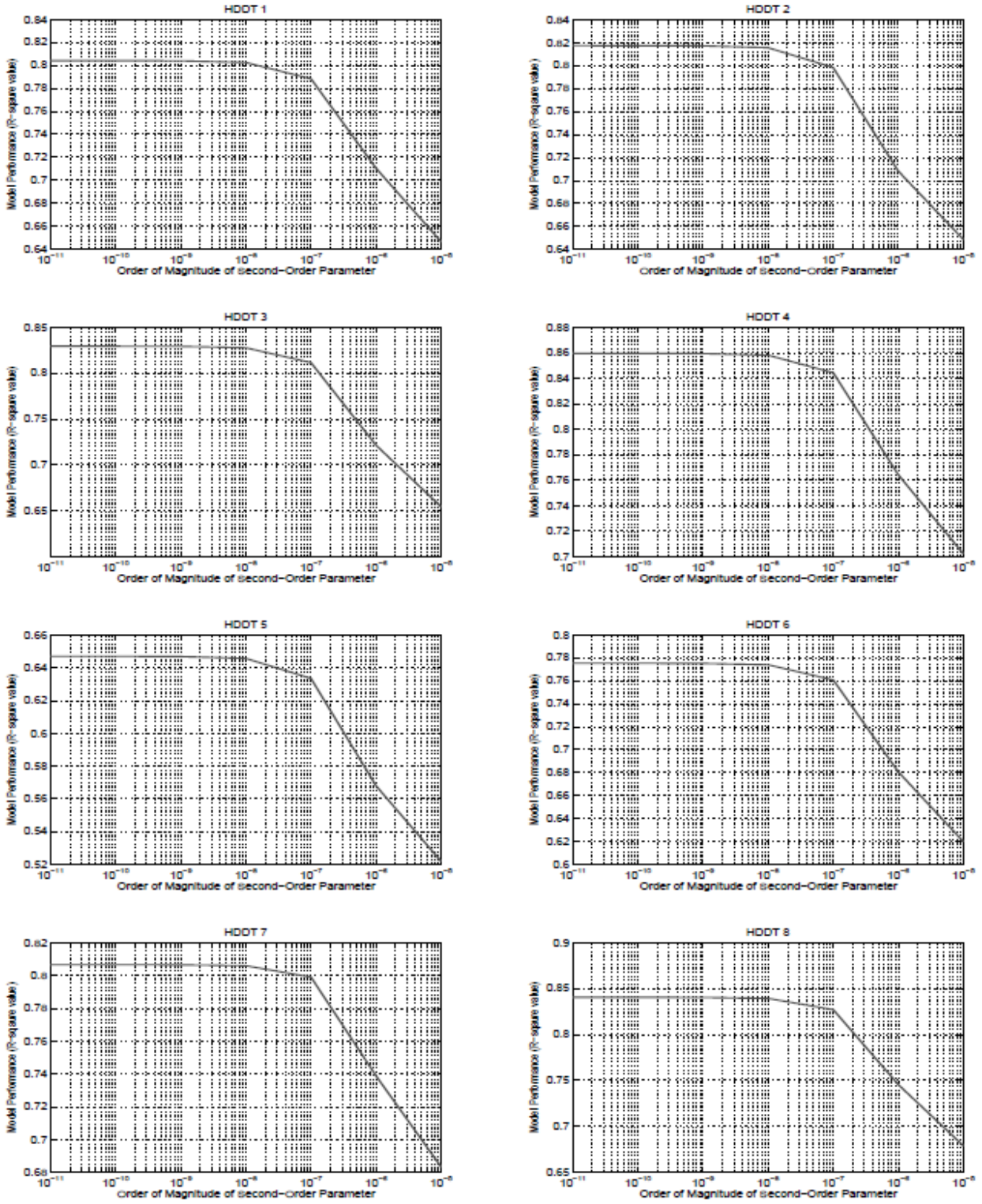

Figure 10: Model performance vs. order of magnitude of the second-order parameter

The effects of road grade and vehicle weight on the optimum fuel economy cruise speed were evaluated for the convex model using the same method. As illustrated in Figure 11, the model produces a bowl-shaped curve as a function of cruise speed and higher road grades result in higher fuel consumption levels, which is similar to LDVs. Specifically, Figure 12 reveals that, when moving downhill, high cruise speeds can minimize fuel consumption levels, yet not recommended for safety purposes. For uphill, steeper roads result in lower optimum cruise speeds, implying that drivers have to reduce their cruise speed to minimize their fuel consumption levels with an increase in the roadway grade.

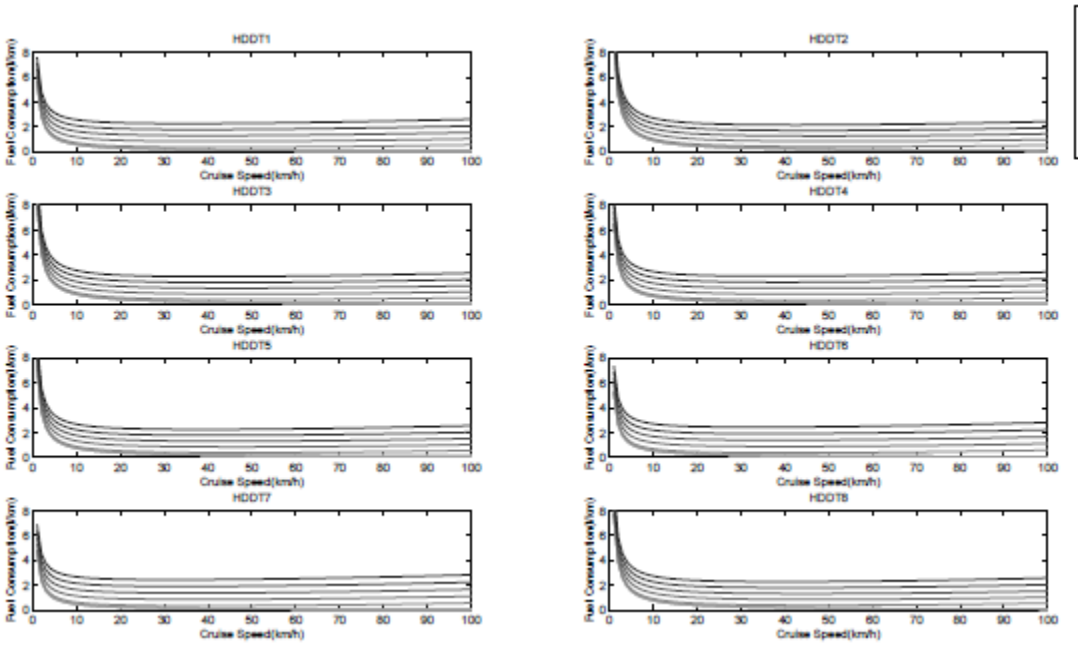

Figure 11 Fuel consumption levels vs. cruise speed at different grade levels (convex model)

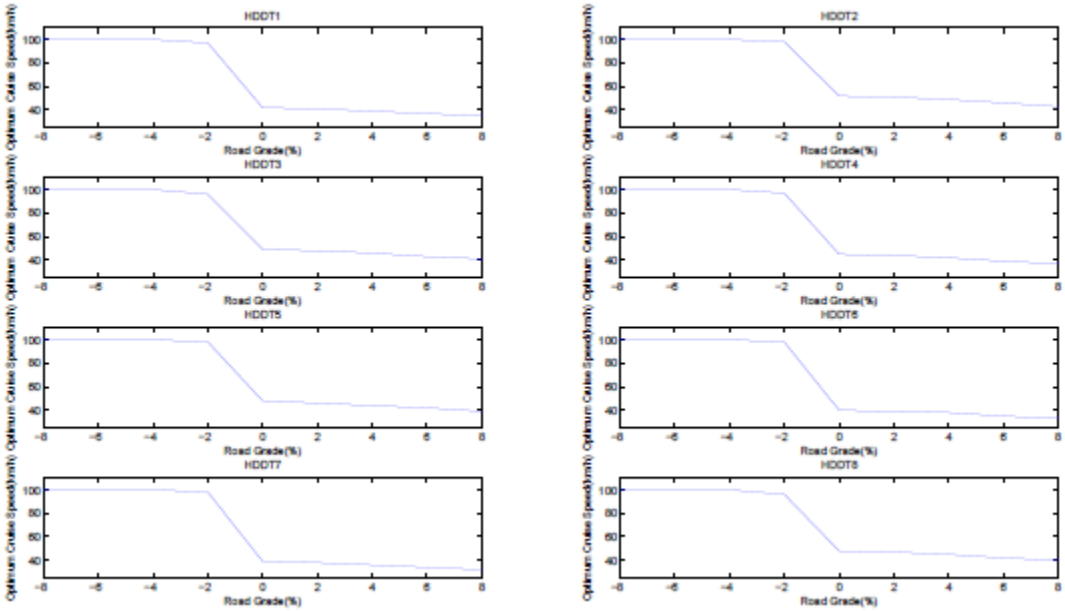

Figure 12 Impacts of road grade on the optimum fuel economy cruise speed

Heavier vehicles, as demonstrated in Figure 13, have higher optimum cruise speeds when moving downhill while lower when moving uphill. It should be noted that, Figure 13-(a), optimum cruise speeds remain constant with an increase in vehicle weight when the road grade is -8%, -6% and -4%. This is because the sensitivity analysis was performed only for the speed range of 0-100 km/h and the optimum cruise speeds already reached the maximum level when vehicle weights were at a low level (e.g. 17,000 kg). Furthermore, Figure 13- (b) clearly indicates that the optimum cruise speeds are more sensitive to vehicle weight at higher grade levels. In short, the convex model can provide reasonable driving recommendations and thus be applicable to eco-driving or eco-routing systems.

Fuel Consumption Model Validation

A rigorous validation procedure was designed using an independent dataset. The validation process was firstly initiated by comparing the model estimates with field measurements along with CMEM and MOVES estimates at an instantaneous fuel consumption level. Furthermore, the variation of fuel estimates over cruise speed was compared between the proposed model and CMEM. Finally, CO2 emissions were computed using fuel estimates and validated against in-field measurements.

Instantaneous Fuel Consumption Validation

Figure 14 provides two example illustrations of the instantaneous model validation, demonstrating that the model estimates in general provide a good agreement with in-field measurements as well as CMEM and MOVES predictions by following the peaks and valleys of the fuel rates. Specifically, Table 9 statistically summarizes the performance of different models. Basically, CMEM performs the best in terms of R^2 values, whereas it produces a bang-bang type of control. Although convex models have a slightly lower R^2 value compared to concave models, they can provide realistic driving recommendations. MOVES performs the worst among the models given that it is designed for conformity use instead of instantaneous analysis; however, it can reflect a large proportion of transient fuel consumption behavior by producing relatively high R^2 values.

Based on the slopes of the regression lines between model estimates and field measurements, all of the models tend to underestimate the fuel consumption levels with slopes smaller than 1.0, whereas the VT-CPFM model produces better approximation to measurements with higher slope values. MOVES has extremely low slope values given that the MOVES database has no trucks as heavy as the combination of the test truck plus the MERL trailer. The researchers at UC Riverside used MERL to collect data which was accounted for as part of truck load, which makes the total truck load extremely high.

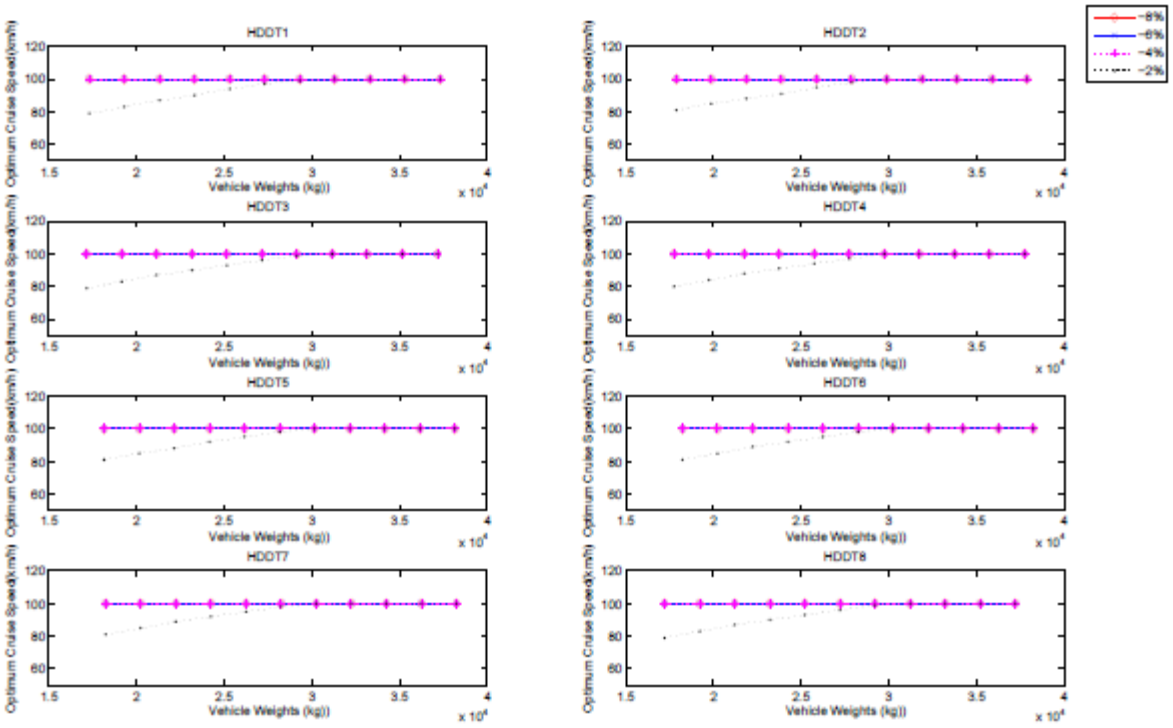

(a) downhill

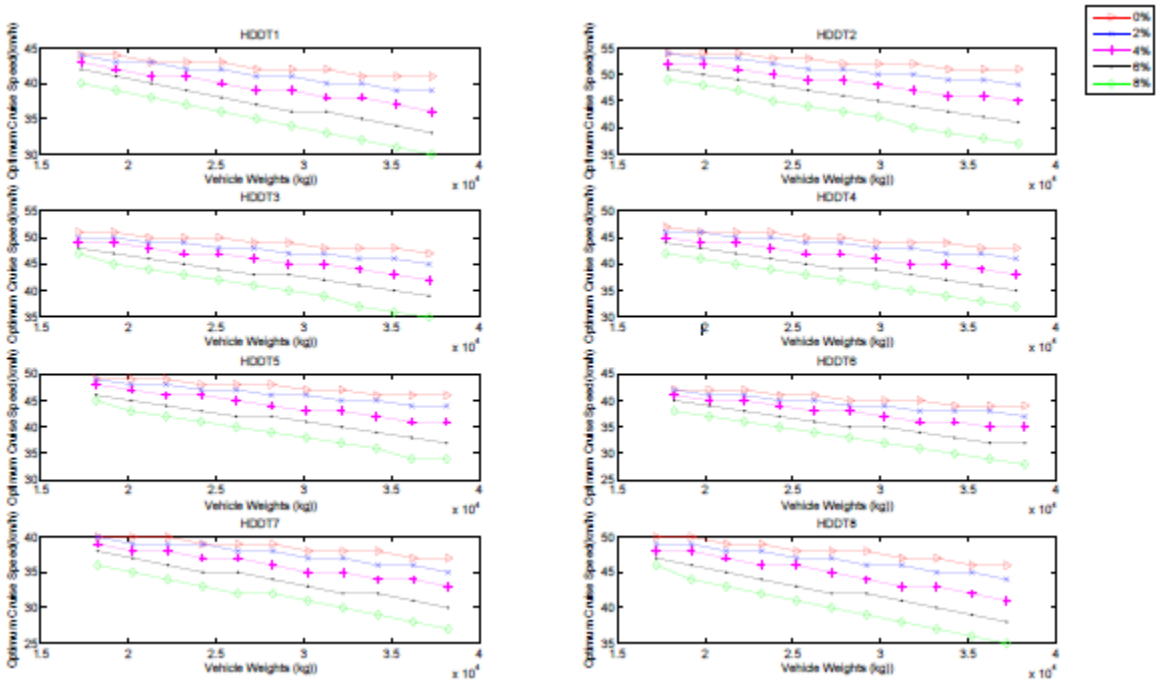

(b) uphill

Figure 13: Impacts of vehicle weight on the optimum fuel economy cruise speed at different grade levels (convex model)

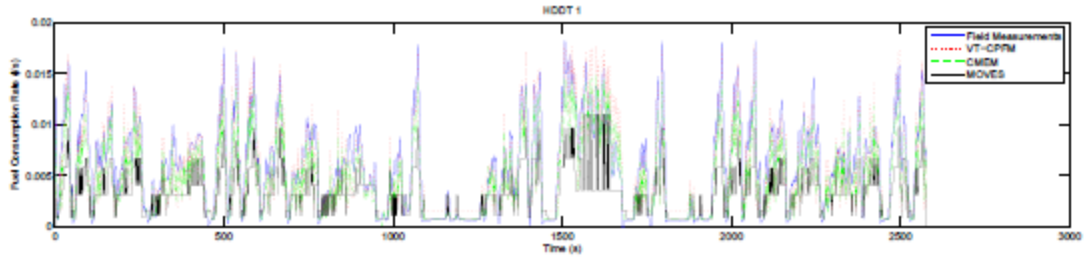

(a) HDDT1

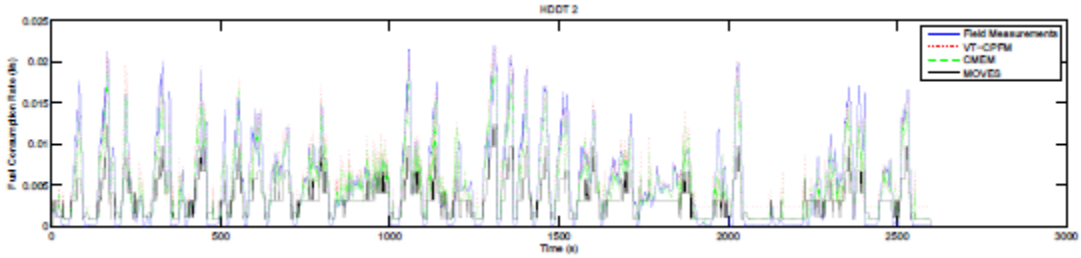

(b) HDDT2

Figure 14: Instantaneous model validation

Table 9: Comparison of model performance

Truck Type	VT-CPFM (concave)		VT-CPFM (convex)		CMEM		MOVES	
	R^2	Slope	R^2	Slope	R^2	Slope	R^2	Slope
HDDT1	0.82	0.93	0.8	0.87	0.87	0.78	0.72	0.42
HDDT2	0.83	0.81	0.81	0.76	0.87	0.75	0.76	0.39
HDDT3	0.84	0.92	0.83	0.81	0.9	0.78	0.77	0.42
HDDT4	0.87	0.91	0.86	0.88	0.9	0.77	0.78	0.42
HDDT5	0.66	0.75	0.64	0.69	0.71	0.65	0.57	0.39
HDDT6	0.78	0.89	0.77	0.86	0.83	0.72	0.72	0.38
HDDT7	0.81	0.82	0.81	0.78	0.85	0.64	0.74	0.35
HDDT8	0.84	0.86	0.84	0.84	0.89	0.79	0.78	0.43

Optimum Cruise Speed

In validating the proposed model, the variation of fuel predictions over cruise speed was compared against CMEM estimates, as illustrated in **Figure *15*** which gives one example result. The two models have highly consistent bowl shaped curves as a function of cruise speed, demonstrating that the proposed model can produce robust fuel estimates. Specifically, the optimum cruise speed ranges between 32-52 km/h (lower than LDVs: 60-80 km/h) for all of the test trucks varying the grade level from 0% to 8%, and moves towards the negative direction with the increase of vehicle load and grade level.

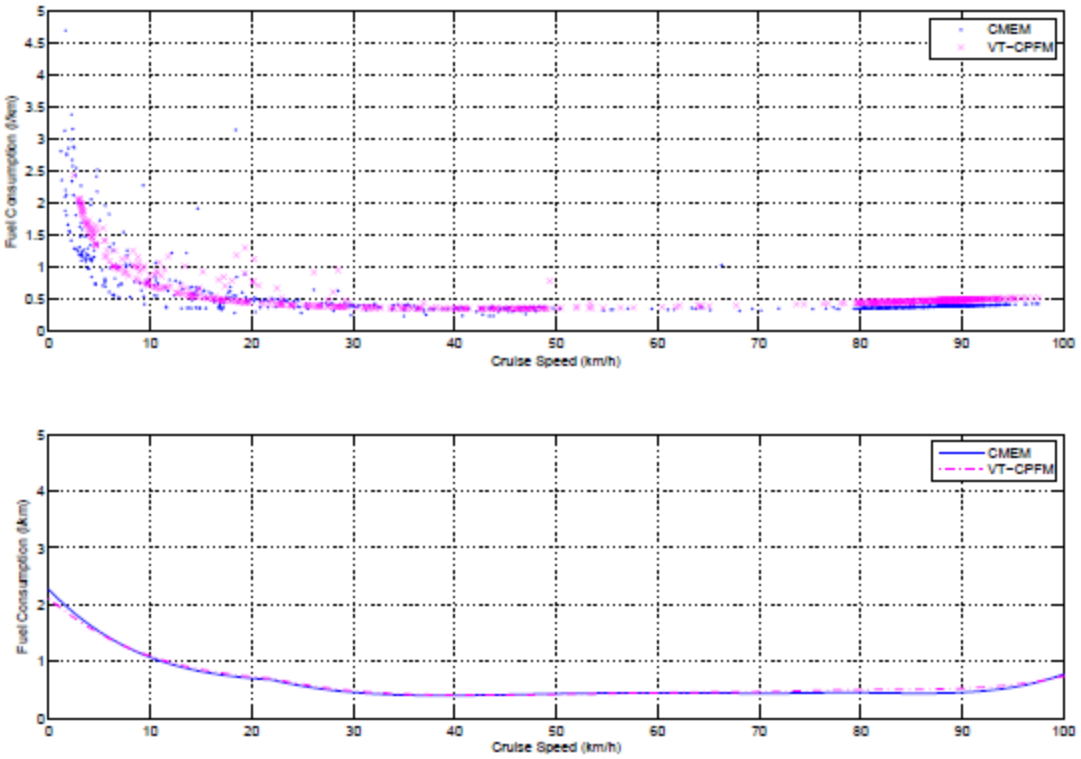

Figure 15: Impact of cruise speed on fuel consumption levels: VT-CPFM vs. CMEM

CO2 Emissions

CO2 can be estimated from the carbon balance equation using the fuel consumption, HC and CO estimates. Given that the magnitude of CO2 emissions is significantly higher than HC and CO emissions, the fuel consumption level is thus the primary factor that affects CO2 emissions. As demonstrated in Rakha, et al. [60], CO2 emission is linearly related to fuel consumption. Equation (46) was used to capture the relationship between CO2 and fuel predictions. The model was firstly calibrated for each truck with CO2 in g/s and fuel consumption in l/s, and the values of θ were then averaged over individual models to generate the average model given that the relationship between CO2 and fuel consumption is only related to fuel type rather than vehicle type. The value of 2070 was used to compute CO2 emissions from fuel consumption estimates. It is found that model estimates are in general consistent with field measurements, as the example results illustrated in Figure 16. The results of other validation efforts are summarized in Table 10 which has an R2 values ranging between 0.74 and 0.85. In general, the model provides reliable CO2 predictions. Noticeably, the model cannot be validated for HDDT 4 and HDDT 5 due to a lack of valid CO2 field measurements, thus the model performance is not discussed for these vehicles.

$$\theta = \frac{CO_2(t)}{FC(t)} \tag{46}$$

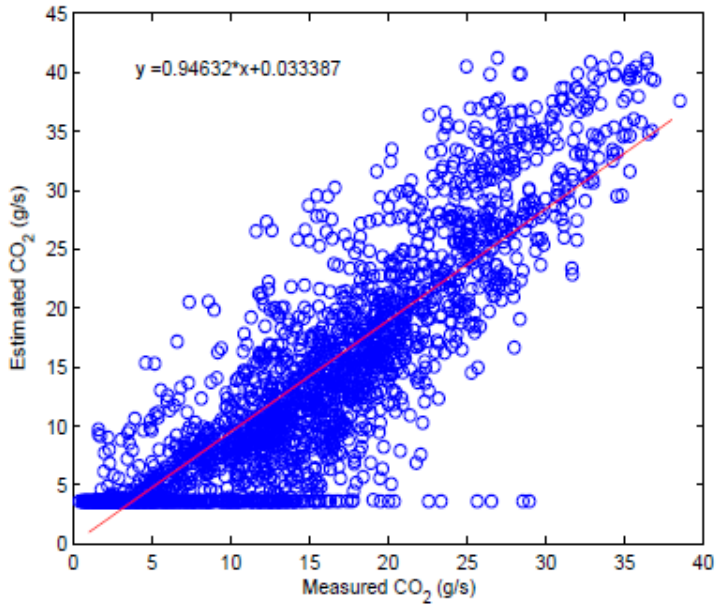

Figure 16: CO2 estimation using fuel consumption model (HDDT 1)

Table 10: The performance of CO2 models

Truck Classification	Coefficients of determination (R^2)	Slope
HDDT 1	0.78	0.95
HDDT 2	0.85	0.72
HDDT 3	0.81	0.82
HDDT 4	NA[a]	NA[a]
HDDT 5	NA[a]	NA[a]
HDDT 6	0.74	0.73
HDDT 7	0.81	0.65
HDDT 8	0.79	0.82

[a]CO_2 model cannot be validated due to the invalid CO_2 in-field measurements.

Emission Model Calibration

Like fuel consumption modeling, each testing truck was individually modeled for the three types of pollutant emissions HC, CO and NOx. A sample modeling result is illustrated in Table 11.

Table 11: Sample Model Coefficients for HDDT 1

Emission	*a*	*b*	*c*	*d*	*e*	*f*	*g*	*h*
CO	-0.023	0.003	58.967	-1.089	-3201.70	70.879	47595	-1209.50
HC	0.035	0.001	11.219	-0.216	-796.41	16.847	22888	-456.31
NO_x	0.049	0.002	100.098	-1.017	-10536.00	161.680	339250	-5640.50

Emission Model Validation

The models were tested using the dataset independent of the calibration data. Due to the space limitation, this report only presents the example results for one truck; namely, HDDT 1. The results are illustrated in Figure 17, Figure 18 and Figure 19 to represent the behavior of

emissions as a function of VT-CPFM fuel consumption and speed. It is found that emissions increase with the increasing fuel consumption, and the highest emission levels occur at the peak of fuel consumption. NOx has the highest level of emissions and is the well-distributed emission compared with CO and HC. NOx makes up the largest portion of diesel emissions at more than 50% because diesel engines are lean combustion engines and the concentration of CO and HC is minimal [71].

The VT-CPFM emission model maintains consistency using the same model to predict emissions. The accuracy of the model was evaluated by estimating the coefficient of determination (R2) of CO, HC, and NOx for the eight trucks. Table 12 shows R2 values for each truck across the three emissions and the average values for each emission. NOx has the highest R2 values, followed by CO then HC, which has the lowest R2 values. Figure 18 illustrates this by showing the well-distributed data for NOx, which were measured more easily and captured more accurately than CO and HC for some trucks. Diesel engines emit low levels of HC [71], making it more difficult to predict accurately compared with NOx. Consequently, NOx has the highest average R2 of 0.857, followed by CO then HC (0.749 and 0.582, respectively).

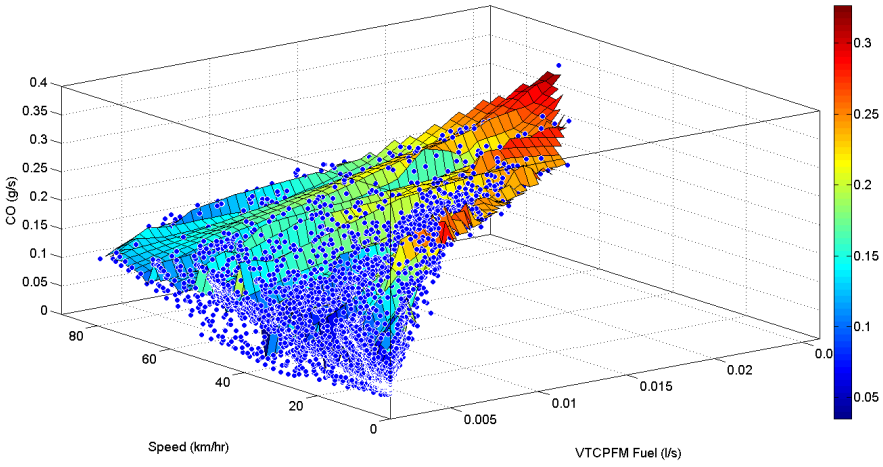

Figure 17: Sample randomized CO emission data with speed and VT-CPFM fuel consumption

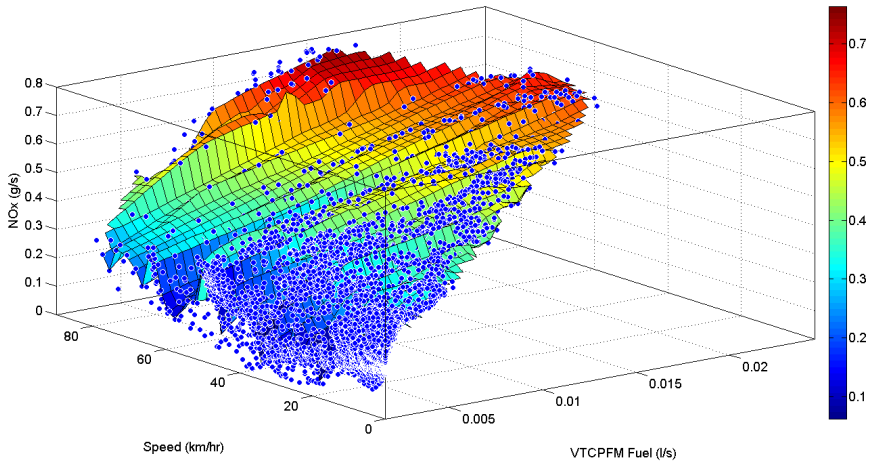

Figure 18: Sample randomized NOx emission data with speed and VT-CPFM fuel consumption

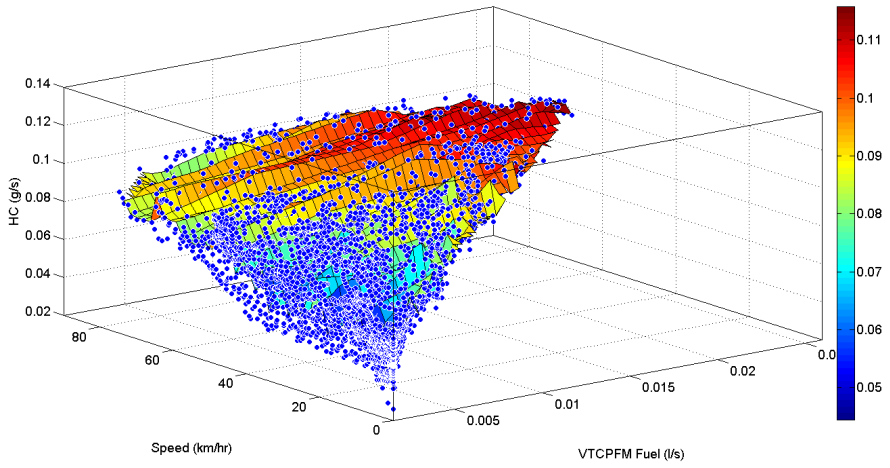

Figure 19: Sample randomized HC emission data with speed and VT-CPFM fuel consumption

Table 12: Coefficient of Determination for Each Truck

Vehicle ID	CO	HC	NOx
HDDT 1	0.752	0.753	0.898
HDDT 2	0.749	0.226	0.821
HDDT 3	0.710	0.583	0.897
HDDT 4	NA	0.651	0.915
HDDT 5	0.721	0.440	0.676
HDDT 6	0.752	0.796	0.858
HDDT 7	0.739	NA	0.862
HDDT 8	0.821	0.626	0.929
Average	0.749	0.582	0.857

The performance of the VT-CPFM emission model was further evaluated and validated by comparing it with CMEM's results Table 13.The predicted emission values were plotted against measured field data to fit the regression line to estimate R2 for each model (Table 13, Figure 20, Figure 21, Figure 22). Table 13 summarizes the individual and average R2 values, revealing the robustness of the model based on its goodness of fit. It is evident that the average R2 values of the VT-CPFM emission model are higher than those for the CMEM model, demonstrating the superior performance of the model. In general, the VT-CPFM model has higher R2 values for almost all the vehicles compared to CMEM.

Table 13: R2 Values for Emission Field Data vs. Estimates for CMEM and VT-CPFM

Vehicle ID	VT-CPFM (CO)	CMEM (CO)	VT-CPFM (HC)	CMEM (HC)	VT-CPFM (NO_x)	CMEM (NO_x)
HDDT 1	0.728	0.586	0.745	0.695	0.924	0.904
HDDT 2	0.779	0.708	0.172	0.148	0.832	0.820
HDDT 3	0.665	0.487	0.566	0.525	0.925	0.951
HDDT 4	NA	NA	0.658	0.512	0.934	0.938
HDDT 5	0.707	0.594	0.423	0.404	0.700	0.661
HDDT 6	0.789	0.645	0.162	0.107	0.880	0.866
HDDT 7	0.743	0.510	NA	NA	0.896	0.824
HDDT 8	0.836	0.613	0.578	0.392	0.955	0.939
Average	0.750	0.592	0.472	0.397	0.881	0.863

The two models are similar in terms of the order of goodness of fit for NOx emissions. Table 13 shows that the average coefficient of determination (R2) NOx emission values for the two models are the highest. Alternatively, the coefficient of determination is the lowest for HC emission estimates. The values imply that NOx has the best fit. VT-CPFM has a slightly higher R2 value than CMEM (0.881 versus 0.863). On the other hand, the average R2 values for HC demonstrate the relatively poor fit between the predicted and measured field data, which is due to the low HC emission levels as mentioned before. Nevertheless, VT-CPFM has better HC estimates than CMEM as expressed in the average R2 values (0.472 versus 0.397). Finally, the VT-CPFM model has a relatively average fit of R2 = 0.750 compared to CMEM with a relatively poor fit of R2 = 0.592 for CO emissions.

The VT-CPFM model is simple, with only eight coefficients and two main parameters, speed and fuel. CMEM requires extensive and complicated data to estimate emissions. For instance, CMEM requires engine speed data, which would require installation of onboard diagnostics to measure. On the other hand, the data used by VT-CPFM are publicly available except for the speed data, which can be easily collected using a GPS device.

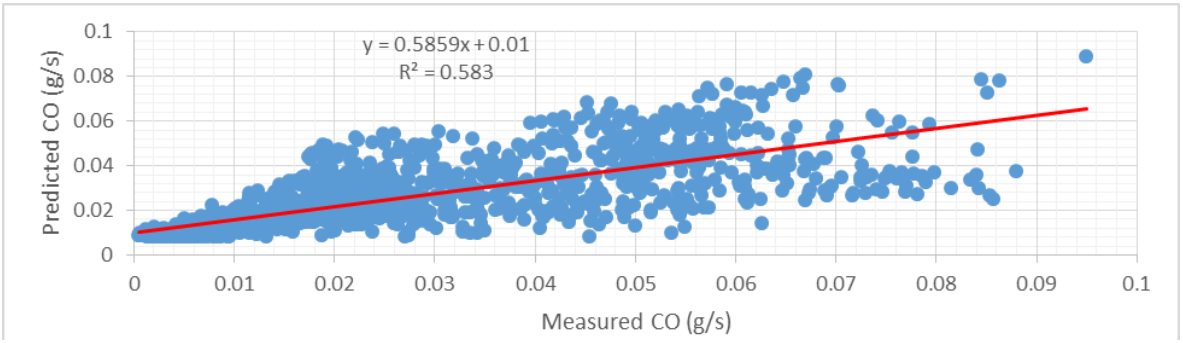

(a) CMEM

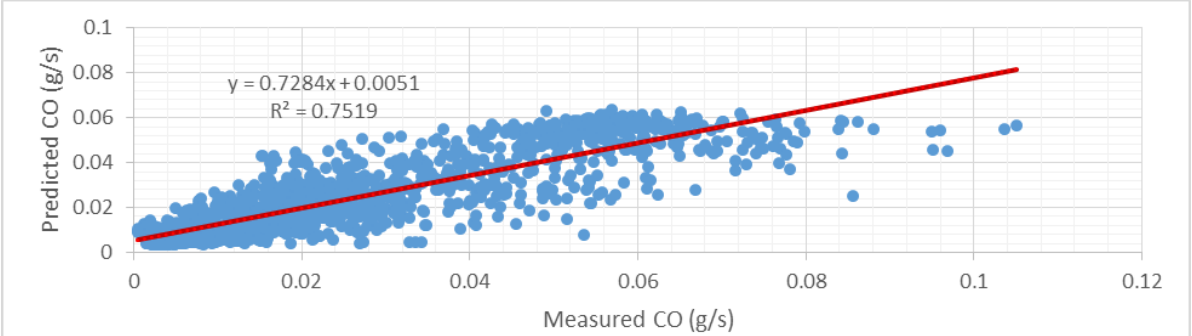

(b) VT-CPFM

Figure 20: Comparison between (a) CMEM and (b) VT-CPFM of CO estimates

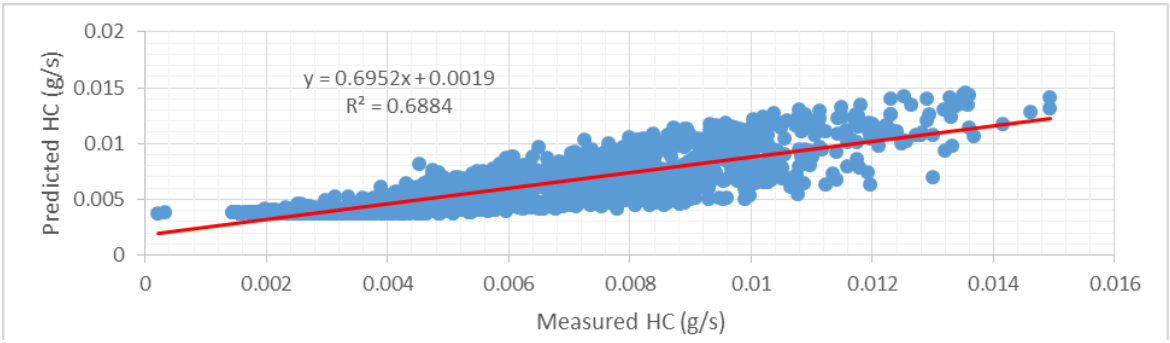

(a) CMEM

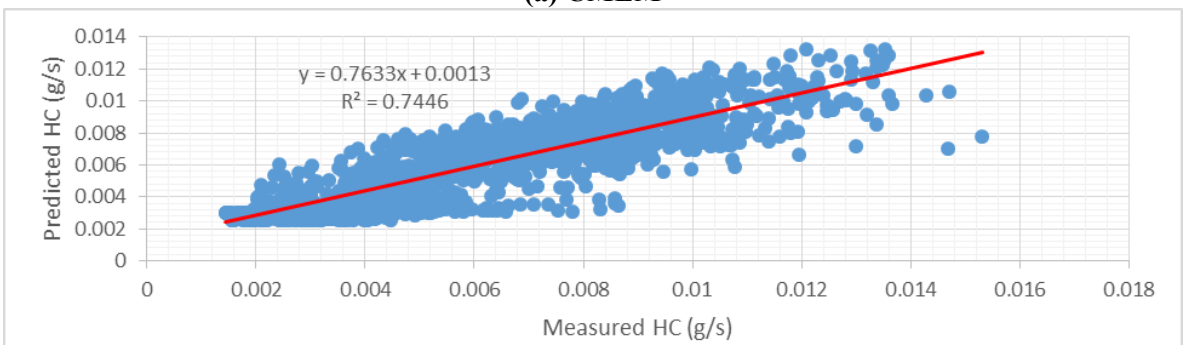

(a) VT-CPFM

Figure 21: Comparison between (a) CMEM and (b) VT-CPFM of HC estimates

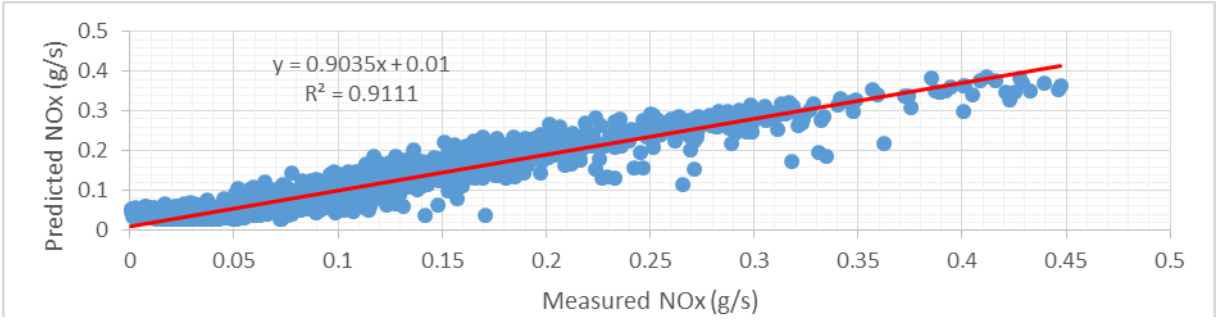

(a) CMEM

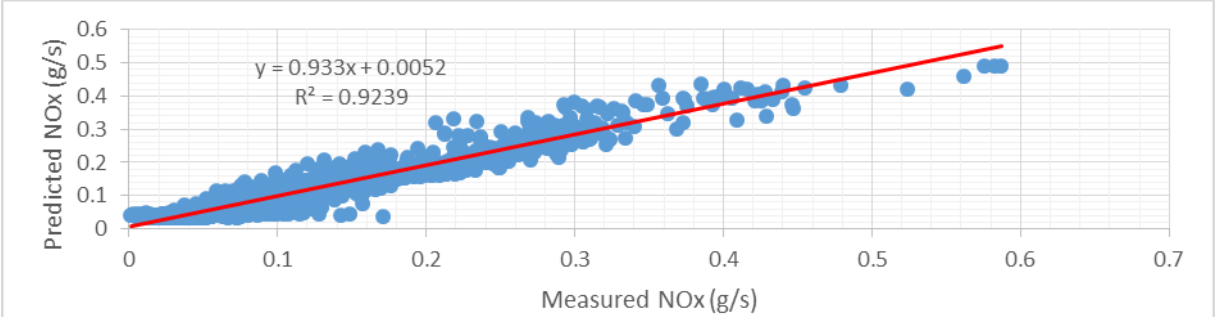

(a) VT-CPFM

Figure 22: Comparison between (a) CMEM and (b) VT-CPFM of NOx estimates

Figure 20, Figure 21, and Figure 22 illustrate the correlation of estimated emissions from CMEM and VT-CPFM with in-field measurements from HDDT 1. NOx, the key target emission and the main concern in HDDT emissions, is highly correlated compared with CO and HC emissions. Moreover, VT-CPFM had better estimates for NOx, CO, and HC compared to CMEM based on the R2 values. The VT-CPFM estimated emissions are uniformly scattered and have better distribution around the regression line than CMEM. This is additional evidence that VT-CPFM provides better fuel estimates than CMEM.

Table 14: Average MAE and SMAPE for CMEM and VT-CPFM

Emissions	CMEM		VT-CPFM	
	MAE	SMAPE	MAE	SMAPE
CO	0.021786	0.54016	0.017014	0.455586
HC	0.000888	0.21699	0.000732	0.193229
NO_x	0.023443	0.24979	0.022614	0.246200

The performance of the model was further investigated and analyzed by estimating mean absolute error (MAE) and symmetric mean absolute percentage error (SMAPE) for CO, HC, and NOx estimates Table 14 and SMAPE were calculated for vehicle trips estimated by the VT-CPFM and CMEM model structure to compute the difference in estimates against in-field measured data. SMAPE can be used as an alternative to mean absolute percentage error (MAPE) when there are zero or near-zero values in the data, which could result in infinitely high error rates that will increase the average error rate and will not represent the correct value. SMAPE was used as benchmark for the two models since some of the emissions values were near-zero. SMAPE yields higher error rates than usual due to the near-zero values but it limits the error to 200% as shown in (47), where A_t is the actual value and F_t is the forecast value at time t.

$$SMAPE = \left| \frac{A_t - F_t}{\frac{A_t + F_t}{2}} \right| \quad (47)$$

NOx had an approximately similar SMAPE for both models, although SMAPE and MAE for CMEM were slightly higher than for VT-CPFM. The HC and CO error rates were higher for CMEM than for VT-CPFM, which corroborates the evident goodness of fit of VT-CPFM over CMEM.

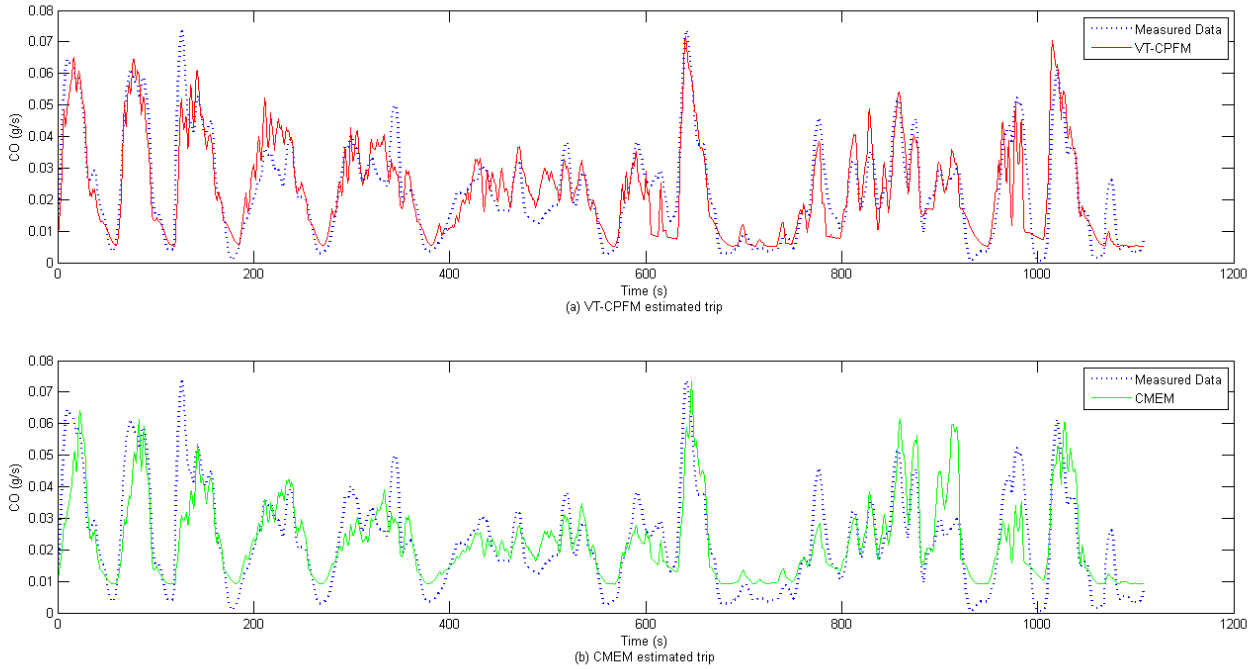

Figure 23: Model validation and comparison with CMEM for CO

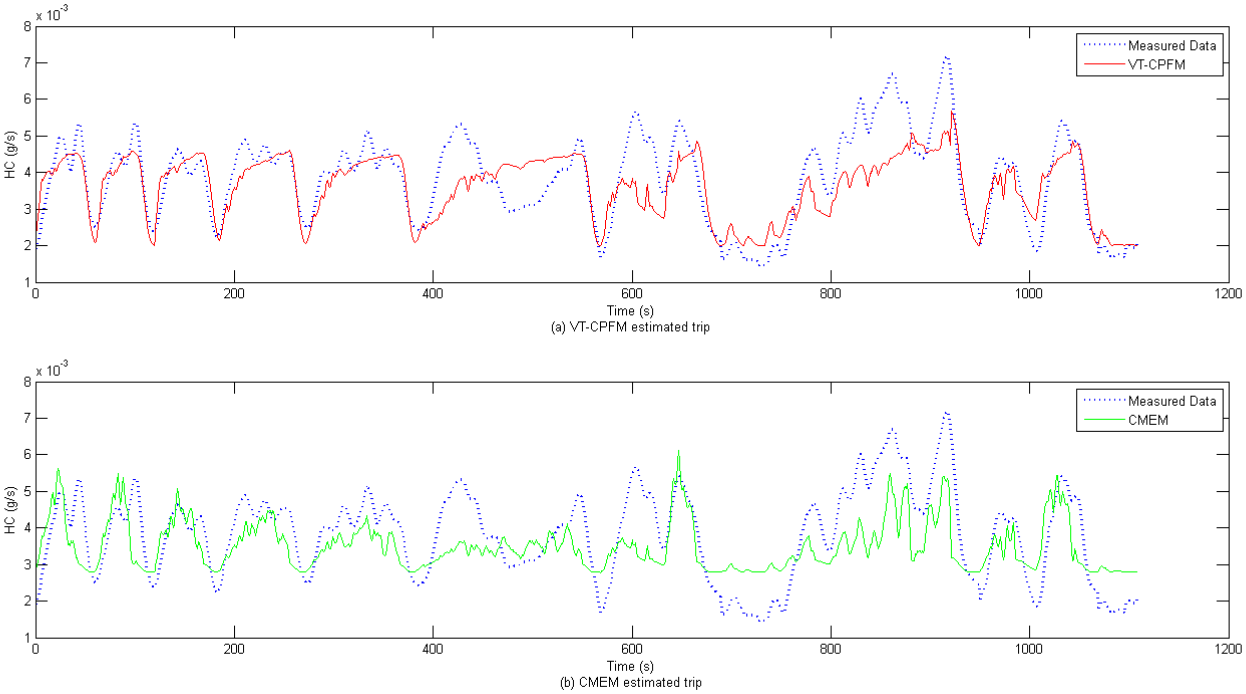

Figure 24: Model validation and comparison with CMEM for HC

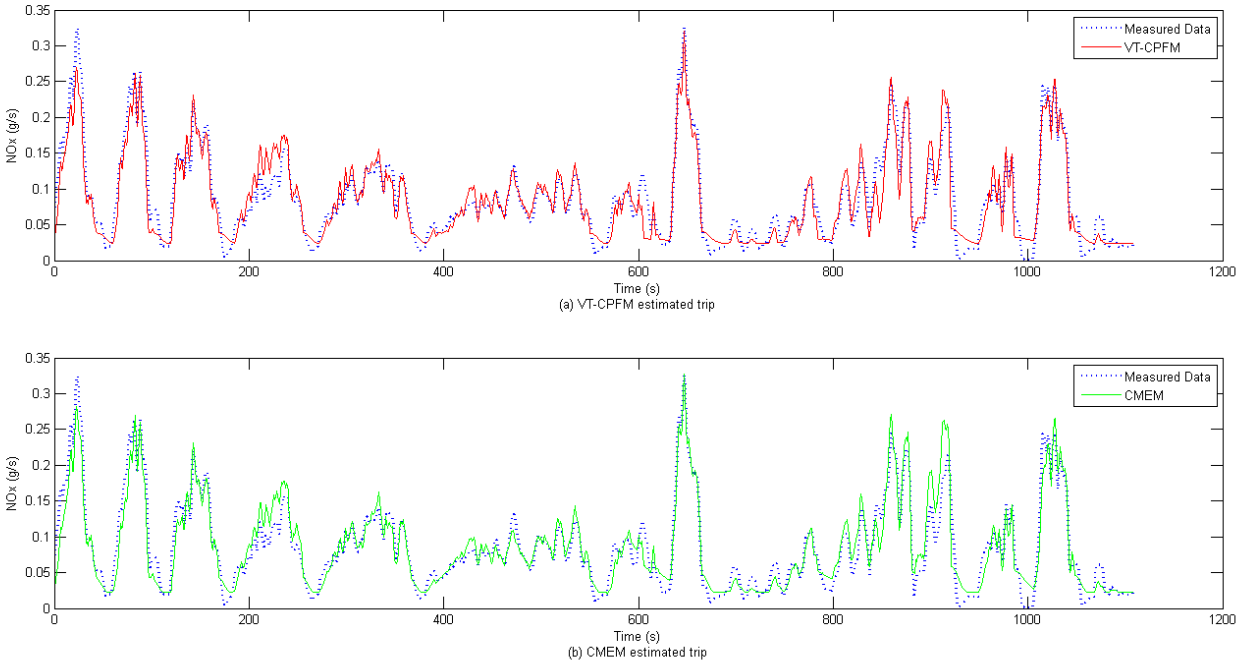

Figure 25: Model validation and comparison with CMEM for NOx

Figure 23, Figure 24, and Figure 25 show sample estimated instantaneous emissions of the two models along with in-field measured data. The figures illustrate the ability of the models to capture the transient behavior of the three pollutants. The high error rates, which correspond to near-zero values are interpreted by the figures showing the large drops in empirical data. For NOx, the two models were similar and fit the measured data well. The VT-CPFM model had better estimates for CO and HC, especially at lower values, where CMEM overestimates the emissions at these values. The VT-CPFM estimates were more consistent with in-field measured data for the three pollutants, specifically for HC and CO, which was expected from the demonstrated goodness of fit of the VT-CPFM model in previous tables and figures.

CONCLUSIONS & RECOMMENDATIONS

The model developed in this paper circumvents the bang-bang type of control in the family of HDDTs fuel consumption and emission modeling. Due to a lack of publicly available data, field measurements are used for model development. The model is calibrated for each individual truck and validated by comparing model estimates against in-field measurements as well as CMEM and MOVES model estimates.

The results of the fuel consumption modeling demonstrate that the model should be restricted to be convex, although empirical measurements do seem to point to a concave function of vehicle power, in order to provide realistic driving recommendations from the system perspective. The convex model is demonstrated to estimate fuel consumption levels consistent with in-field measurements as well as CMEM and MOVES, without significantly sacrificing the model accuracy. The optimum fuel economy cruise speed ranges between 32-52 km/h for all of the test vehicles varying the grade level from 0% to 8%, and moves towards the negative direction with an increase in the vehicle load and grade level; namely, steeper roadway grades and heavier vehicles result in lower optimum cruise speeds. The fuel predictions of the model can accurately estimate CO2 emissions, which are demonstrated to be consistent with field measurements.

The results of the emission modeling demonstrate that the pollutant emissions, HC, CO, NOx, can be mathematically formulated as a polynomial function of fuel consumption and vehicle speed. The developed emission models are demonstrated to generate results consistent with in-field measurements, especially for NOx model which produces a better fit compared to CO and HC. The model is also demonstrated to provide better performance than CMEM in terms of the coefficient of determination.

It is recommended that EPA require HDDTs to report their fuel economy in the future so that the model can be calibrated using publicly available data without mass in-field data collection, which can maximize the cost-effectiveness of model development

APPENDIX

APPENDIX A. PER-TRIP HAULAGE UNIT COST FUNCTION

A-1. Truck System

The original equations for truck and rails were obtained from Janic [12].

Cost (USD dollars) = $\alpha \times (d^1)^{\beta} \times X$, where α = 5.46 and β = -0.278.

S^{11} = 1 TEU $\quad C^1(X, d^1, S^{11}) = 1.2 \times \frac{\alpha}{2} \times (d^1)^{\beta+1} \times X$

S^{12} = 2 TEU $\quad C^1(X, d^1, S^{12}) = \frac{\alpha}{2} \times (d^1)^{\beta+1} \times X$

S^{13} = 3 TEU $\quad C^1(X, d^1, S^{13}) = 0.9 \times \frac{\alpha}{2} \times (d^1)^{\beta+1} \times X$

A-2. Rail System

The original equations for truck and rails were obtained from Janic [26].

Cost (USD dollars) = $\alpha \times (W^v \times d^2)^{\beta} \times d^2 \times X$, where α = 5.46, β = 0.74, and W^v (total weight of a train) = W_0^V (locomotive weight) + W_1^V (flatcars weight) + X_{ij} × 14.3 (loads weight) for v type of train.

S^{21} = 60 TEU $\quad C^2(X, d^2, S^{21}) = 1.07 \times [0.58 \times \{89 + 20 \times 24 + X \times 14.3) \times d_{ij}^2\}^{0.74}] \times d_{ij}$

S^{22} = 75 TEU $\quad C^2(X, d^2, S^{22}) = 1.07 \times [0.58 \times \{89 + 25 \times 24 + X \times 14.3) \times d_{ij}^2\}^{0.74}] \times d_{ij}$

S^{23} = 144 TEU $\quad C^2(X, d^2, S^{23}) = 1.07 \times [0.58 \times \{(89 \times 2 + 48 \times 24 + X \times 14.3) \times d_{ij}^2\}^{0.74}] \times d_{ij}$

A-3. Vessel System

The haulage cost of vessels was estimated using the equation developed by [10].

S^{31} = 200 TEU $\quad C^3(X, d^3, S^{31}) = 1.07 \times 0.8^b \times 0.08 \times (1/1.609) \times d^3 \times X = 0.04 \times d^3 \times X$

S^{32} = 500 TEU $\quad C^3(X, d^3, S^{32}) = 1.07 \times 0.8 \times 0.05 \times (1/1.609) \times d^3 \times X = 0.025 \times d^3 \times X$

S^{33} = 800 TEU $\quad C^3(X, d^3, S^{31}) = 1.07 \times 0.8 \times 0.04 \times (1/1.609) \times d^3 \times X = 0.02 \times d^3 \times X$

APPENDIX B. PER-TRIP UNIT COST FUNCTIONS OF FUEL CONSUMPTIONS

B-1. Truck and Rail System

The total fuel consumptions of heavy trucks and rails (in gallon) are calculated using the formula developed by Barth and Boriboonsomsin [27].

$FR\ (g) = \phi \cdot d(k \cdot N \cdot V + P/\eta)/(44 \cdot v)$

where,

P (total engine power (kW)) = $d(M \cdot a + M \cdot g \cdot \sin\theta + 0.5 \cdot C_d \cdot \rho \cdot A \cdot v^2 + M \cdot g \cdot C_r \cdot \cos\theta) / (1000 \cdot \eta_{tf}) + (P_{acc} \cdot d / v)$,

Φ = fuel-to-air mass ratio

d = traveling distance (m)

k = engine friction factor (typically 0.2)

V = engine displacement (liters, typically between 2 and 8)

N = engine speed (in rpm)

η = efficiency parameter for diesel engines (typically 0.4)

v = speed (m/s)

M = weight (kg)

a = acceleration (m/s^2)

g = gravitational constant (m/s^2, typically 9.81)

ρ = air density (kg/m^3, typically 1.2041)

A = frontal surface area (m^2, typically between 2.1 and 5.6)

C_d = coefficient of aerodynamic drag (typically 0.7)

C_r = coefficient of rolling resistance (typically 0.01)

η_{tf} = vehicle drive train efficiency (typically 0.4)

P_{acc} = engine power demand associated with running losses of the engine and the operation of vehicle accessories such as usage of air conditioning (typically 0)

B-2. Vessel System

The per-trip fuel consumptions of vessels were calculated using the formula developed by [28].

$$FS = \left[MF \cdot \left(\frac{s_1}{s_0} \right)^3 + AF \right] \cdot \frac{d}{24 s_1}$$

where,

MF = main engine(s) daily fuel consumption (MF = 206 g/kWh)

AF = auxiliary engine(s) daily fuel consumption (AF = 221g/kWh)

s_1 = operational speed of vessel (in nautical miles)

s_0 = design at-sea speed of vessel (in nautical miles)

d = traveling distance (nautical miles)

The MF = 206 g/kWh and AF = 221g/kWh were used based on the activity assumptions

REFERENCES

[1] V. Roso, J. Woxenius, and K. Lumsden, "The dry port concept: connecting container seaports with the hinterland," *Journal of Transport Geography,* vol. 17, pp. 338-345, 2009.

[2] A. Jaržemskis and A. V. Vasiliauskas, "Research on dry port concept as intermodal node," *Transport,* vol. 22, pp. 207-213, 2007.

[3] A. Beresford, S. Pettit, Q. Xu, and S. Williams, "A study of dry port development in China," *Maritime Economics & Logistics,* vol. 14, pp. 73-98, 2012.

[4] X. Qiu, G. Q. Huang, and J. S. L. Lam, "A bilevel analytical model for dynamic storage pricing in a Supply Hub in Industrial Park (SHIP)," *IEEE Transactions on Automation Science and Engineering,* vol. 12, pp. 1017-1032, 2015.

[5] D. Pacanovsky, C. Jahren, R. Palmer, R. Newman, and D. Howland, "A decision support system to load containers to double-stack rail cars," *Civil Engineering Systems,* vol. 11, pp. 247-261, 1995.

[6] M. Lang, J. Przybyla, and X. Zhou, "Loading containers on double-stack cars: Multi-objective optimization models and solution algorithms for improved safety and reduced maintenance cost."

[7] Y.-C. Lai, C. P. Barkan, and H. Önal, "Optimizing the aerodynamic efficiency of intermodal freight trains," *Transportation Research Part E: Logistics and Transportation Review,* vol. 44, pp. 820-834, 2008.

[8] ZIM. *ZIM's Container Guide*. Available: http://www.zim.com/knowledgecenter/containers/documents/container_guide.pdf

[9] P. Arnold, D. Peeters, and I. Thomas, "Modelling a rail/road intermodal transportation system," *Transportation Research Part E: Logistics and Transportation Review,* vol. 40, pp. 255-270, 2004.

[10] K. Cullinane and M. Khanna, "Economies of scale in large container ships," *Journal of transport economics and policy,* pp. 185-207, 1999.

[11] M. W. Horner and M. E. O'Kelly, "Embedding economies of scale concepts for hub network design," *Journal of Transport Geography,* vol. 9, pp. 255-265, 2001.

[12] M. Janic, "Modelling the full costs of an intermodal and road freight transport network," *Transportation Research Part D: Transport and Environment,* vol. 12, pp. 33-44, 2007.

[13] N. Kim, M. Janic, and B. Van Wee, "Trade-off between carbon dioxide emissions and logistics costs based on multiobjective optimization," *Transportation Research Record: Journal of the Transportation Research Board,* pp. 107-116, 2009.

[14] M. E. O'Kelly and D. Bryan, "Hub location with flow economies of scale," *Transportation Research Part B: Methodological,* vol. 32, pp. 605-616, 1998.

[15] I. Racunica and L. Wynter, "Optimal location of intermodal freight hubs," *Transportation Research Part B: Methodological,* vol. 39, pp. 453-477, 2005.

[16] P. Sitek and J. Wikarek, "Mathematical programming model of cost optimization for supply chain from perspective of logistics provider," *Management and Production Engineering Review,* vol. 3, pp. 49-61, 2012.

[17] D. Skorin-Kapov, J. Skorin-Kapov, and M. O'Kelly, "Tight linear programming relaxations of uncapacitated p-hub median problems," *European Journal of Operational Research,* vol. 94, pp. 582-593, 1996.

[18] R. Hillestad, "Optimization problems subject to a budget constraint with economies of scale," *Operations Research,* vol. 23, pp. 1091-1098, 1975.
[19] D. J. Graham, A. Couto, W. E. Adeney, and S. Glaister, "Economies of scale and density in urban rail transport: effects on productivity," *Transportation Research Part E: Logistics and Transportation Review,* vol. 39, pp. 443-458, 2003.
[20] S. R. Jara-Dıaz and L. J. Basso, "Transport cost functions, network expansion and economies of scope," *Transportation Research Part E: Logistics and Transportation Review,* vol. 39, pp. 271-288, 2003.
[21] N. S. Kim, B. Park, and K.-D. Lee, "A knowledge based freight management decision support system incorporating economies of scale: multimodal minimum cost flow optimization approach," *Information Technology and Management,* vol. 17, pp. 81-94, 2016.
[22] U. S. E. P. Agency, "Inventory of U.S. Greenhouse Gas Emissions and Sinks: 1990 – 2013," U.S. Environmental Protection Agency2015.
[23] C. f. C. a. E. Solutions, "Center for Climate and Energy Solutions," 2016.
[24] U. S. E. P. Agency, "Final Rulemaking to Establish Greenhouse Gas Emissions Standards and Fuel Efficiency Standards for Medium- and Heavy-Duty Engines and Vehicles."
[25] U. S. E. P. Agency. (2016). *Smart Way*. Available: http://www3.epa.gov/smartway/
[26] M. Janic, "An assessment of the performance of the European long intermodal freight trains (LIFTS)," *Transportation Research Part A: Policy and Practice,* vol. 42, pp. 1326-1339, 2008.
[27] M. Barth, T. Younglove, and G. Scora, "Development of a heavy-duty diesel modal emissions and fuel consumption model," *California Partners for Advanced Transit and Highways (PATH),* 2005.
[28] J. J. Corbett, H. Wang, and J. J. Winebrake, "The effectiveness and costs of speed reductions on emissions from international shipping," *Transportation Research Part D: Transport and Environment,* vol. 14, pp. 593-598, 2009.
[29] M. Matlab, "Natick, MA: Mathworks," 1999.
[30] S. C. Davis, S. W. Diegel, and R. G. Boundy, "Transportation energy data book," 2008.
[31] A. EPA, "Inventory of US greenhouse gas emissions and sinks: 1990-2009," EPA 430-R-11-0052011.
[32] J. Yanowitz, R. L. McCormick, and M. S. Graboski, "In-use emissions from heavy-duty diesel vehicles," *Environmental Science & Technology,* vol. 34, pp. 729-740, 2000.
[33] W. Harrington and A. Krupnick, "Improving Fuel Economy in Heavy-Duty Vehicles," *Resources for the Future DP,* pp. 12-02, 2012.
[34] K. Dzenisiuk, "Eco-driving-changing truck driver behavior to achieve long-term sustainability results," *Master's thesis,* 2012.
[35] F. Lattemann, K. Neiss, S. Terwen, and T. Connolly, "The predictive cruise control: A system to reduce fuel consumption of heavy duty trucks," *SAE transactions,* vol. 113, pp. 139-146, 2004.
[36] E. Pindilli, "Applications for the Environment: RealTime Information Synthesis (AERIS) Benefit-Cost Analysis," *Prepared by United States Department of Transportation, Federal Highway Administration Office,* 2012.

[37] Y. Takada, S. Ueki, A. Saito, N. Sawazu, and Y. Nagatomi, "Improvement of fuel economy by eco-driving with devices for freight vehicles in real traffic conditions," SAE Technical Paper 0148-7191, 2007.
[38] K. Ahn and H. A. Rakha, "Network-wide impacts of eco-routing strategies: a large-scale case study," *Transportation Research Part D: Transport and Environment,* vol. 25, pp. 119-130, 2013.
[39] K. Boriboonsomsin, M. J. Barth, W. Zhu, and A. Vu, "Eco-routing navigation system based on multisource historical and real-time traffic information," *Intelligent Transportation Systems, IEEE Transactions on,* vol. 13, pp. 1694-1704, 2012.
[40] H. Rakha, K. Ahn, and K. Moran, "Integration framework for modeling eco-routing strategies: Logic and preliminary results," *International Journal of Transportation Science and Technology,* vol. 1, pp. 259-274, 2012.
[41] K. Ahn, H. Rakha, and K. Moran, "ECO-cruise control: Feasibility and initial testing," in *Transportation Research Board 90th Annual Meeting*, 2011.
[42] J. N. Barkenbus, "Eco-driving: An overlooked climate change initiative," *Energy Policy,* vol. 38, pp. 762-769, 2010.
[43] Y. Saboohi and H. Farzaneh, "Model for developing an eco-driving strategy of a passenger vehicle based on the least fuel consumption," *Applied Energy,* vol. 86, pp. 1925-1932, 2009.
[44] D. L. Schall and A. Mohnen, "Incentivizing energy-efficient behavior at work: An empirical investigation using a natural field experiment on eco-driving," *Applied Energy,* 2015.
[45] S. Soylu, "The effects of urban driving conditions on the operating characteristics of conventional and hybrid electric city buses," *Applied Energy,* vol. 135, pp. 472-482, 2014.
[46] J. Guo, Y. Ge, L. Hao, J. Tan, Z. Peng, and C. Zhang, "Comparison of real-world fuel economy and emissions from parallel hybrid and conventional diesel buses fitted with selective catalytic reduction systems," *Applied Energy,* vol. 159, pp. 433-441, 2015.
[47] N. C. Onat, M. Kucukvar, and O. Tatari, "Conventional, hybrid, plug-in hybrid or electric vehicles? State-based comparative carbon and energy footprint analysis in the United States," *Applied Energy,* vol. 150, pp. 36-49, 2015.
[48] W. S. Wayne, N. N. Clark, R. D. Nine, and D. Elefante, "A comparison of emissions and fuel economy from hybrid-electric and conventional-drive transit buses," *Energy & fuels,* vol. 18, pp. 257-270, 2004.
[49] M. Balat and H. Balat, "Recent trends in global production and utilization of bio-ethanol fuel," *Applied energy,* vol. 86, pp. 2273-2282, 2009.
[50] A. Demirbas, "Importance of biodiesel as transportation fuel," *Energy policy,* vol. 35, pp. 4661-4670, 2007.
[51] J. M. López, Á. Gómez, F. Aparicio, and F. J. Sánchez, "Comparison of GHG emissions from diesel, biodiesel and natural gas refuse trucks of the City of Madrid," *Applied Energy,* vol. 86, pp. 610-615, 2009.
[52] D. C. Rakopoulos, C. D. Rakopoulos, and E. G. Giakoumis, "Impact of properties of vegetable oil, bio-diesel, ethanol and n-butanol on the combustion and emissions of turbocharged HDDI diesel engine operating under steady and transient conditions," *Fuel,* vol. 156, pp. 1-19, 2015.

[53] U. EPA, "User's Guide to MOBILE6. 1 and MOBILE6. 2," *Environmental Protection Agency,* 2003.
[54] K. Ahn and H. Rakha, "The effects of route choice decisions on vehicle energy consumption and emissions," *Transportation Research Part D: Transport and Environment,* vol. 13, pp. 151-167, 2008.
[55] H. Rakha, K. Ahn, and A. Trani, "Development of VT-Micro model for estimating hot stabilized light duty vehicle and truck emissions," *Transportation Research Part D: Transport and Environment,* vol. 9, pp. 49-74, 2004.
[56] S. Hausberger, M. Rexeis, M. Zallinger, and R. Luz, "PHEM User guide for version 10," *TUG/FVT Report,* pp. 1-57, 2010.
[57] R. Smit, R. Smokers, and E. Rabé, "A new modelling approach for road traffic emissions: VERSIT+," *Transportation Research Part D: Transport and Environment,* vol. 12, pp. 414-422, 2007.
[58] M. Barth, F. An, T. Younglove, C. Levine, G. Scora, M. Ross*, et al.*, *Development of a comprehensive modal emissions model*: National Cooperative Highway Research Program, Transportation Research Board of the National Academies, 2000.
[59] M. Barth, G. Scora, and T. Younglove, "Modal emissions model for heavy-duty diesel vehicles," *Transportation Research Record: Journal of the Transportation Research Board,* pp. 10-20, 2004.
[60] H. A. Rakha, K. Ahn, K. Moran, B. Saerens, and E. Van den Bulck, "Virginia tech comprehensive power-based fuel consumption model: model development and testing," *Transportation Research Part D: Transport and Environment,* vol. 16, pp. 492-503, 2011.
[61] S. Park, H. Rakha, K. Ahn, and K. Moran, "Virginia Tech Comprehensive Power-based Fuel Consumption Model (VT-CPFM): Model Validation and Calibration Considerations," *International Journal of Transportation Science and Technology,* vol. 2, pp. 317-336, 2013.
[62] J. Wang and H. A. Rakha, "Fuel consumption model for conventional diesel buses," *Applied Energy,* vol. 170, pp. 394-402, 2016.
[63] J. Wang and H. A. Rakha, "Hybrid-Electric Bus Fuel Consumption Modeling: Model Development and Comparison to Conventional Buses," in *Transportation Research Board 95th Annual Meeting*, 2016.
[64] H. Rakha, I. Lucic, S. H. Demarchi, J. R. Setti, and M. V. Aerde, "Vehicle dynamics model for predicting maximum truck acceleration levels," *Journal of transportation engineering,* vol. 127, pp. 418-425, 2001.
[65] J. W. Fitch, "Motor truck engineering handbook," *Technology,* vol. 2004, pp. 03-08, 1994.
[66] J. Y. Wong, *Theory of ground vehicles*: John Wiley & Sons, 2001.
[67] W. Edwardes and H. Rakha, "Virginia Tech Comprehensive Power-Based Fuel Consumption Model: Modeling Diesel and Hybrid Buses," *Transportation Research Record: Journal of the Transportation Research Board,* pp. 1-9, 2014.
[68] C. Feng, "Transit bus load-based modal emission rate model development," 2007.
[69] D. R. Cocker, S. D. Shah, K. Johnson, J. W. Miller, and J. M. Norbeck, "Development and application of a mobile laboratory for measuring emissions from diesel engines. 1.

Regulated gaseous emissions," *Environmental science & technology,* vol. 38, pp. 2182-2189, 2004.

[70] S. Park, H. Rakha, K. Ahn, and K. Moran, "Predictive eco-cruise control: Algorithm and potential benefits," in *Integrated and Sustainable Transportation System (FISTS), 2011 IEEE Forum on*, 2011, pp. 394-399.

[71] İ. A. Reşitoğlu, K. Altinişik, and A. Keskin, "The pollutant emissions from diesel-engine vehicles and exhaust aftertreatment systems," *Clean Technologies and Environmental Policy,* vol. 17, pp. 15-27, 2015.